

62-604

FACILITY FORM 602	N65 18099 (ACCESSION NUMBER)	(THRU)
	112 (PAGES)	(CODE)
	CR-57080 (NASA CR OR TMX OR AD NUMBER)	14 (CATEGORY)

FINAL ENGINEERING REPORT
MARINER R FLUXGATE MAGNETOMETER

JPL Contract 950185

R. Kobayashi
D. Sassa

GPO PRICE \$ _____
OTS PRICE(S) \$ _____
Hard copy (HC) \$4.00
Microfiche (MF) \$0.25

105 pages

16 March 1962

MARSHALL LABORATORIES
3530 Torrance Boulevard
Torrance, California

*This work was performed for the Jet Propulsion
Laboratory, California Institute of Technology, sponsored by the
National Aeronautics and Space Administration under
contract NAS 7-100*

ACKNOWLEDGEMENTS

The authors wish to express their gratitude to all the Jet Propulsion Laboratory and Marshall Laboratories personnel who contributed maximum effort in developing the Mariner R Triaxial Fluxgate Magnetometer.

The following is the Final Engineering Report on the Mariner R Triaxial Fluxgate Magnetometer which was designed, developed and fabricated by Marshall Laboratories (ML) under Jet Propulsion Laboratories (JPL) Contract 950185.

The primary objective of the program was to design and construct a triaxial fluxgate magnetometer to measure interplanetary magnetic vector fields. Secondary objectives were (1) perform in-flight calibration upon command, (2) provide precision regulated power for the magnetometer electronics, and (3) monitor the unit temperature.

The magnetometer portion of the unit consists of a set of three probes mounted in an orthogonal manner in an integrated package to measure three mutually perpendicular components of the magnetic field vector, and a set of electronic circuits which provide probe drive current, detect the probe outputs and conditions them for transmission over the data link. The data output signal is biased at + 3.5v d-c for zero field and plus or minus 2.5v full scale deviation from the bias level for plus or minus field variations, respectively.

Automatic scale switching circuits provide two ranges of measurement; ± 64 gamma, and ± 320 gamma. One output is used to indicate the range of measurement being made. That is 64 gamma scale is identified by a high level (+ 12v d-c), 320 gamma scale is identified by a low level (+ 0.3v d-c).

In-flight calibration upon command is designed into the unit. A calibrated field of 32 gamma is generated by passing current through the probe auxiliary windings to determine scale one sensitivity. The circuit is designed to require a command signal to reset itself to normal operation at the end of the calibration period.

Primary power available on the spacecraft is 100 volts peak-to-peak square wave at 2400 cps. A stable precision regulator converts the primary a-c power to + 12.00v d-c with a stability of $\pm 0.2\%$ and -9.0v d-c $\pm 5\%$ with a stability of $\pm 0.2\%$.

In the design of the highly sensitive magnetometer, a test volume is required that is shielded against earth's magnetic field and man-made disturbances. This required the use of a 30" high by 12-1/2" diameter cylindrical fluxtank and a 48" diameter spherical fluxtank developed in the Mariner A program. The cylindrical tank

allowed versatility of single axis operation while the spherical tank, housing a triaxial Helmholtz coil array, allowed triaxial operation for complete unit test.

An adapter unit was designed to be used in conjunction with a portable checkout suitcase, developed for Mariner A, to provide output monitor devices and to simulate all command signals. The suitcase is used to verify performance of the magnetometer unit in a go-no-go manner during bench or environmental test.

The magnetometer unit was successfully designed, fabricated and tested. Final test results are included in Appendix C.

TABLE OF CONTENTS

	Page
INTRODUCTION	1
SYSTEM DESCRIPTION	1
EQUIPMENT DESCRIPTION	5
Flight Electronics	5
Sensor	5
Magnetometer Electronics	8
Power Supply	24
Package Design	27
Special Purpose Equipment	32
Cylindrical Fluxtank	32
Spherical Fluxtank	37
Checkout Suitcase and Adapter Unit	44
TESTING AND CALIBRATION	50
Pre-Calibration Adjustments	51
Final Calibration	51
SUMMARY	52
APPENDICES	
A. SENSOR ANALYSIS	54
B. TEST PROCEDURES	63
C. FINAL TEST RESULTS	86

ILLUSTRATIONS

Figure		Page
1	Magnetometer unit peripheral functional data	3
2	Magnetometer functional system block diagram	4
3	Triaxial fluxgate magnetometer sensor	6
4	Triaxial fluxgate magnetometer block diagram	9
5	Monoaxial fluxgate magnetometer schematic diagram	10
6	Oscillator characteristic curves	12
7	Second harmonic band pass filter characteristics	14
8a	Functional diagram of scale switching network	16
8b	Basic circuit	16
8c	Field-switch relation	16
9	Basic phase control network	19
10a	Basic phase detector circuit	21
10b	Functional diagram	21
10c	Relative waveforms	21
11	In-flight calibrate and null field circuit schematic	23
12	In-flight calibration command signal and readout time	25
13	Precision regulated power supply, +12v d-c and -9v d-c, schematic diagram	26
14	Final flight electronics unit	31

Figure		Page
15	Final flight sensor unit	31
16	Cylindrical fluxtank internal assemblies	35
17	Cylindrical fluxtank, model ML 102-1	36
18a	Stairstep generator circuit	38
18b	Equivalent circuit	38
19	Spherical fluxtank, model ML 103-2	40
20	Dual Helmholtz coil form	42
21	Functional diagram of spherical fluxtank control unit for one axis. All axes are identical.	43
22	Lower hemisphere of spherical fluxtank, Helmholtz coil, sensor fixture, and sensor	45
23	Checkout adapter unit schematic diagram	47
24	Block diagram of checkout suitcase system	49
25	Flux-current relation	56
26	Probe sensitivity versus drive current curve	62

INTRODUCTION

The following is the Final Engineering Report of the Mariner R Triaxial Fluxgate Magnetometer submitted by Marshall Laboratories, Torrance, California, to the Jet Propulsion Laboratory in fulfillment of Contract 950185.

In general, the report contains detailed technical discussions related to electrical design, test, and calibration process.

Special purpose equipment used in this contract is also described since they are essential parts of the over-all system operation.

Sensor analysis is presented in Appendix A. Appendix B contains test procedures and Appendix C contains final test results and the master drawing list.

SYSTEM DESCRIPTION

Since the Mariner R Magnetometer was a modification of the Mariner A Magnetometer, much of this report is similar to the latter final report.

Figure 1 shows the Magnetometer Unit peripheral signals. The Magnetometer Unit, capable of several functional operations, consists of two basic subunits integrated into two housing. Figure 2 is a simplified system block diagram which shows the inter-relation of the subunits.

The sensor consists of three fluxgate probes mounted orthogonally in an integrated package to measure three mutually perpendicular components of the magnetic field vector. An auxiliary winding is wound on each probe to provide a means for generating in-flight calibration and nulling ambient magnetic fields.

The magnetometer electronics subsystem supplies probe drive current, detects the vector magnetic field sensor signals, and converts them to d-c voltage outputs. Automatic scale switching provides two linear scales of measurement; ± 64 gamma and ± 320 gamma. Upon command from the DAS, in-flight calibration is performed. This calibration is performed by generating approximately 32 gamma by passing a known current through the sensor auxiliary windings.

Primary power from the spacecraft is 2400 cps square wave voltage. A transformer full wave bridge rectifier converts the a-c to d-c voltage

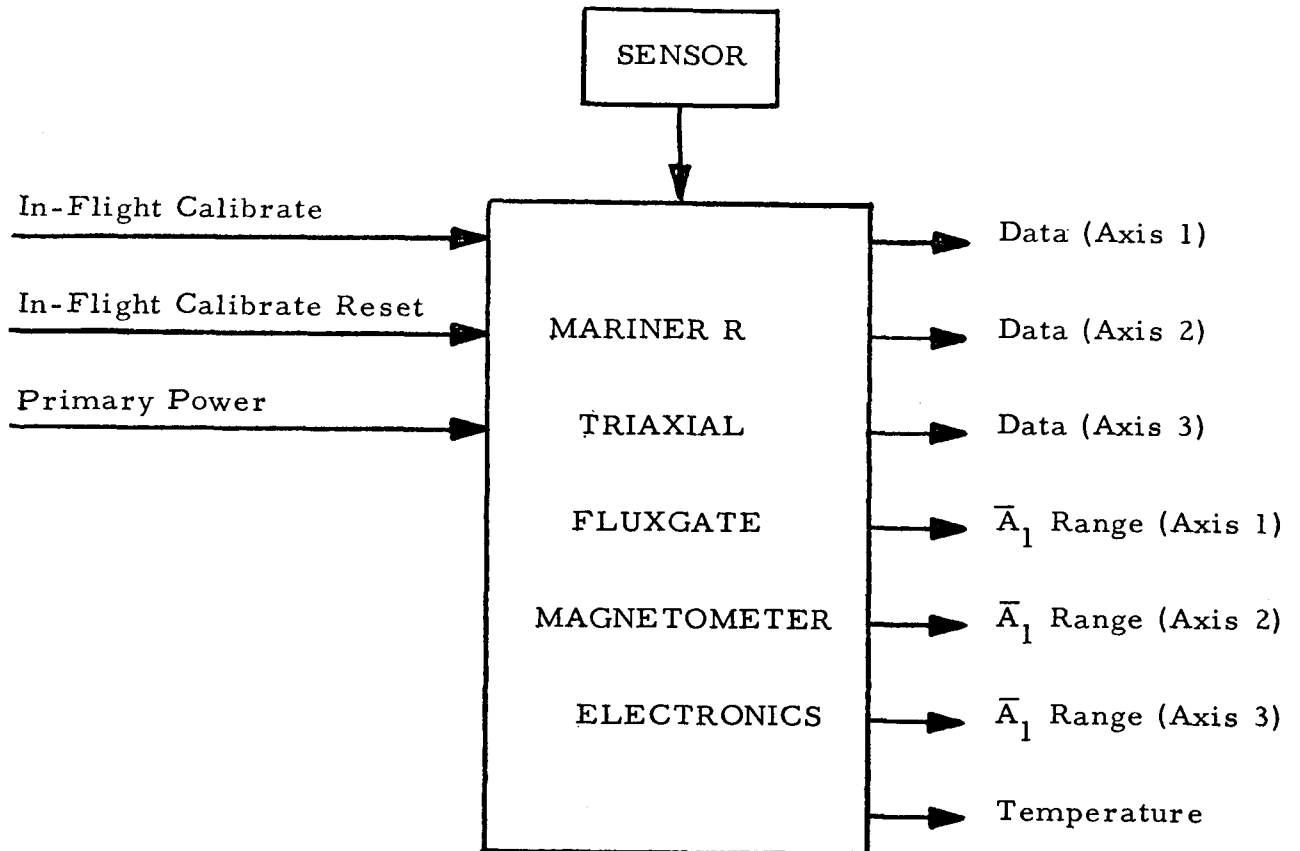


Figure 1. Magnetometer unit peripheral functional data.

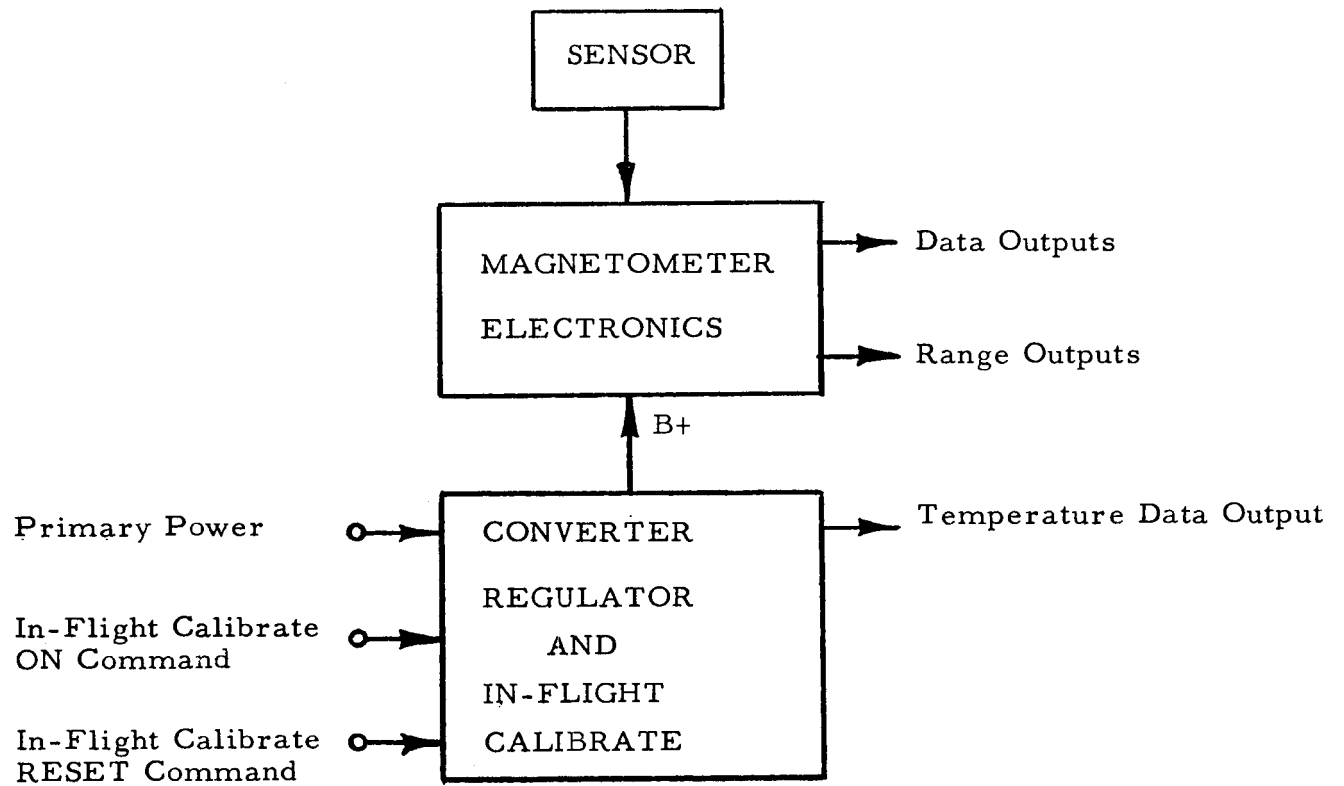


Figure 2. Magnetometer functional system block diagram.

which if followed by a precision series regulator. Regulation is critical in order to maintain stability and accuracy compatible with measurement requirements and analog-to-digital conversion resolution.

EQUIPMENT DESCRIPTION

Two general categories of equipment designed for this project are the flight electronics and special purpose equipment.

Flight Electronics.

The flight unit consists of three basic subunits; sensor, magnetometer, and power supply. Marshall Laboratories developed all the electronics associated with the unit except the sensor which was supplied by JPL. However, since the sensor is a major part of the system, a brief discussion is presented to illustrate the principle of measurement.

Sensor: The sensor, which is compatible with the fluxgate electronics, is designed and fabricated by Institut Dr. Förster in Reutlingen, Germany and is shown in Figure 3.

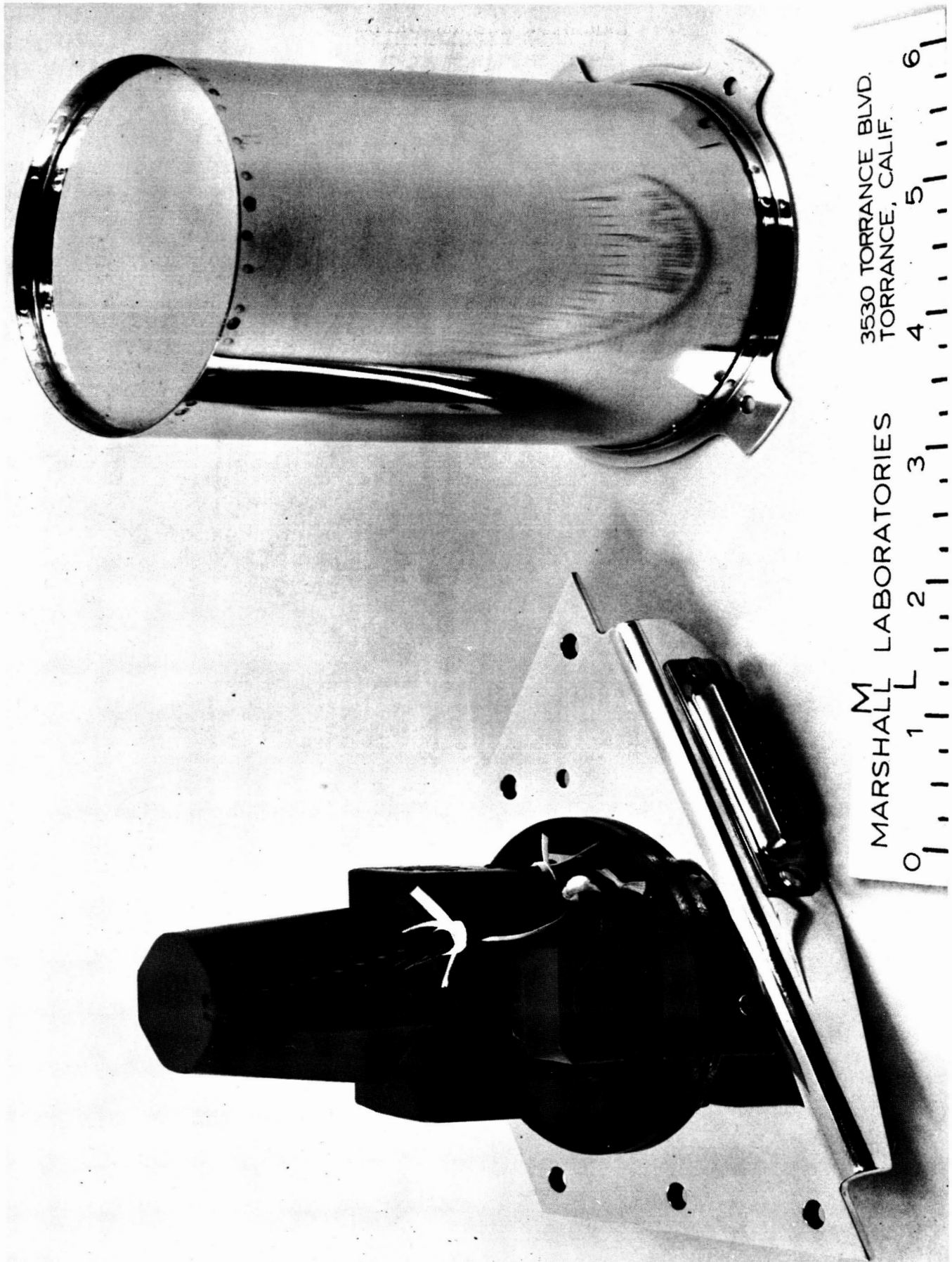


Figure 3. Triaxial Fluxgate Magnetometer Sensor.

A single axis sensor consists of two high permeability cores whose primary windings are connected in series opposing and secondary windings in series aiding. The cores are driven symmetrically into saturation by an a-c magnetic field produced by the primary winding drive current. With no external magnetic field present, the sum of the induced secondary voltages is zero. The presence of an external magnetic field parallel to the sensor axis creates a static magnetic bias that destroys the symmetry of the drive waveform. Fourier analysis of the resultant waveform shows that the amplitude of the second harmonic component is proportional to the magnitude of the axial field component and drive frequency. The phase of the second harmonic component is proportional to the polarity or direction of the field. That is,

$$e_o = K\omega H \sin 2\omega t$$

where K is a lumped constant. A brief mathematical analysis is presented in Appendix A. With special techniques, the tripole orthogonal sensor is constructed such that cross coupling of drive fields between axes is negligible. An auxiliary winding is provided for generating calibration fields.

The following is the sensor specifications.

1. Sensitivity: $10 \mu \text{ v}/\gamma$
2. Stability factor: 0.25γ for ± 1 oersted exposure
3. Frequency: 20 Kc fundamental
4. Power: 100 mw/axis
5. Crosstalk: 1 part in 10^4
6. Auxiliary coil constant: $0.5 \mu \text{ a}/\gamma$
7. Axis orientation accuracy: 0.1 degree
8. Total weight including housing hardware: 0.67 lbs.

Magnetometer Electronics: Figure 4 shows the block diagram of the triaxial fluxgate magnetometer. Sheet 1 of ML drawing 50227 shows the detailed schematic diagram. The simplified circuit is shown in Figure 5 for reference for the following technical discussion.

Since the amplitude of the second harmonic signal is dependent upon operating frequency, a stable oscillator is required. A grounded base oscillator operating at the sensor second harmonic frequency ($2f$) is employed, whose frequency determining factor is, approximately,

$$(2\omega)^2 = \frac{1}{LC}$$

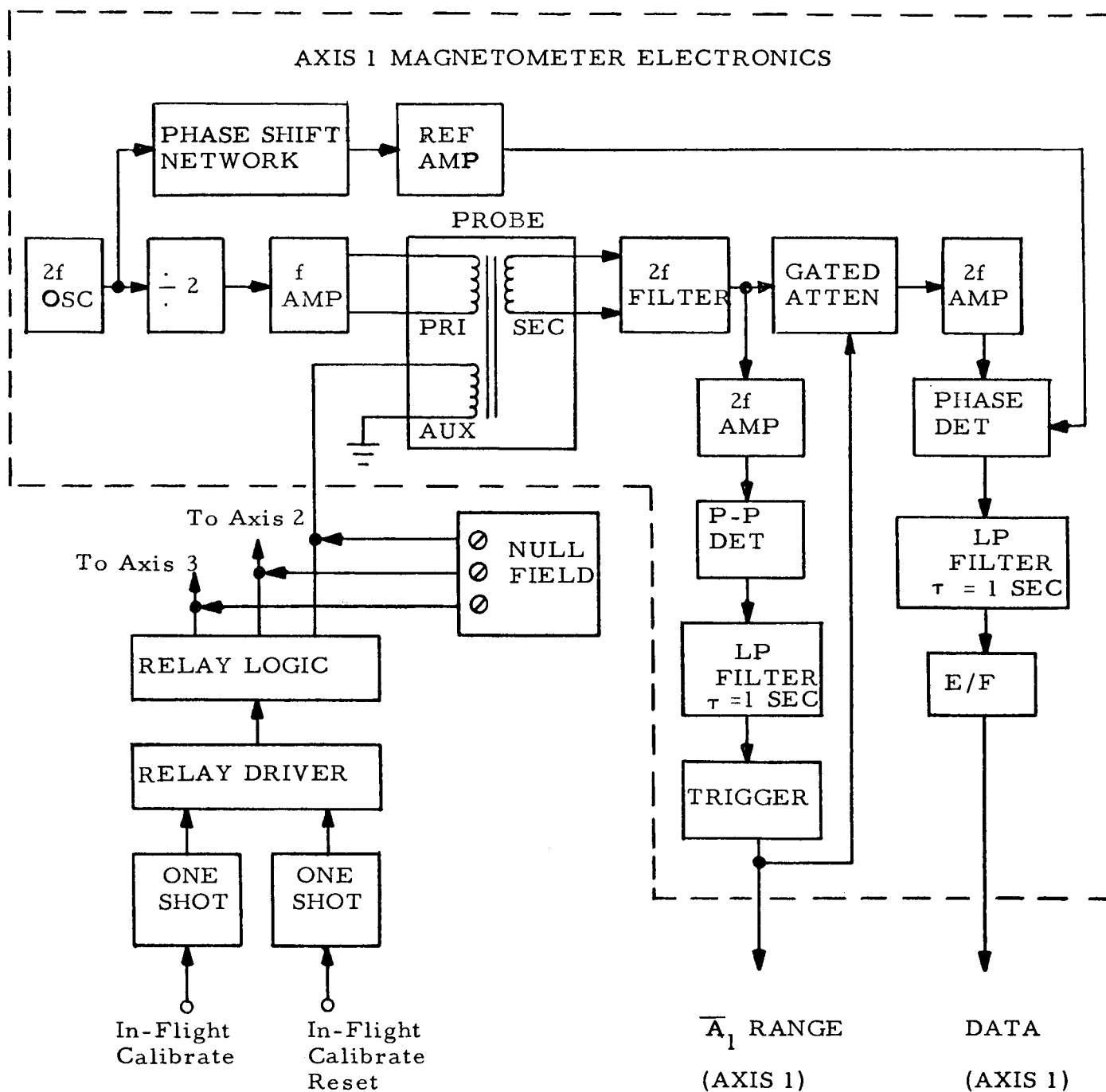


Figure 4. Triaxial fluxgate magnetometer block diagram.

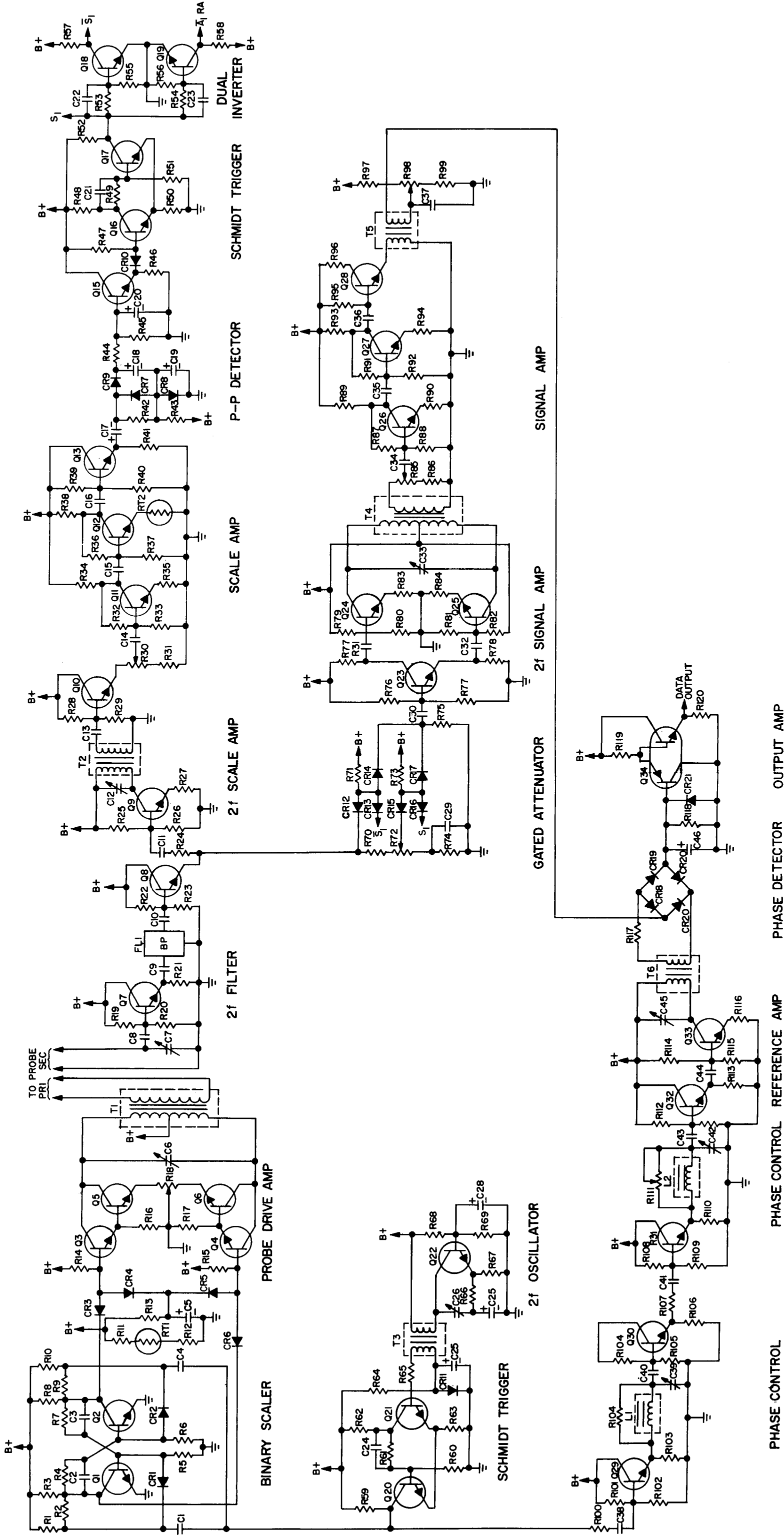


Figure 5. Monoaxial Fluxgate Magnetometer Schematic Diagram.

where

$$C = C26$$

$$L = T3 \text{ primary winding inductance}$$

Hence, frequency stability is only dependent upon passive LC elements and stability of better than $\pm 0.1\%$ between 0°F and $+125^{\circ}\text{F}$ is obtained (see Figure 6). Stability of frequency with supply voltage is also shown where $\pm 4\%$ change in supply voltage results in only about $\pm 0.2\%$ change in frequency.

The primary considerations of the probe driving function are that frequency and amplitude remain constant and the waveform maintains full wave symmetry: that is,

$$e(\omega t) = -e(\omega t + \pi)$$

Full wave symmetry insures that there is no second harmonic component in the probe primary which may couple to the secondary and cause erroneous zero field offset. The oscillator design fulfills the frequency stability requirement. A binary countdown technique is employed, to obtain the fundamental probe drive frequency, automatically insuring symmetrical duty cycle. Also this approach conveniently yields a reference signal ($2f$) for phase detection. Since the output of the oscillator is a distorted sine wave, waveshaping is first performed

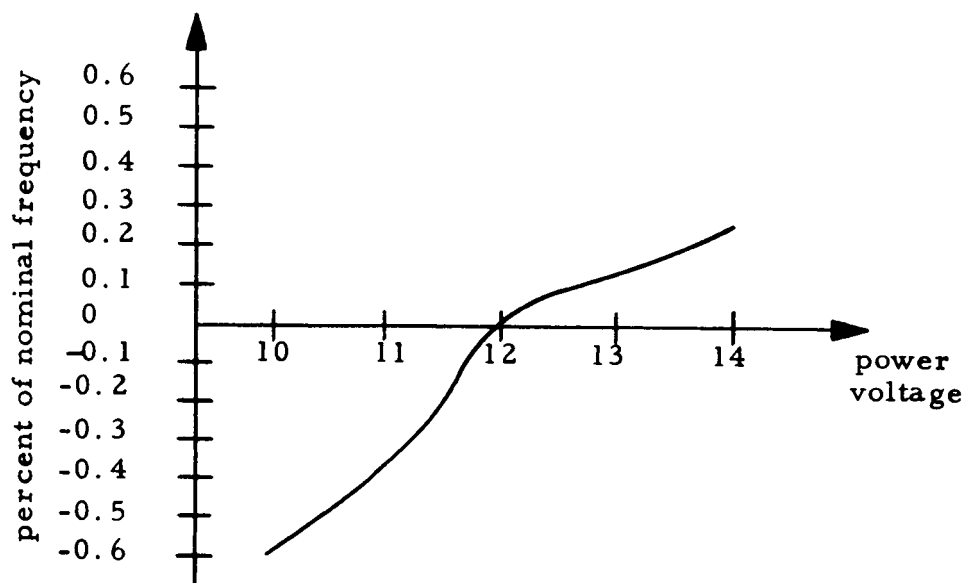
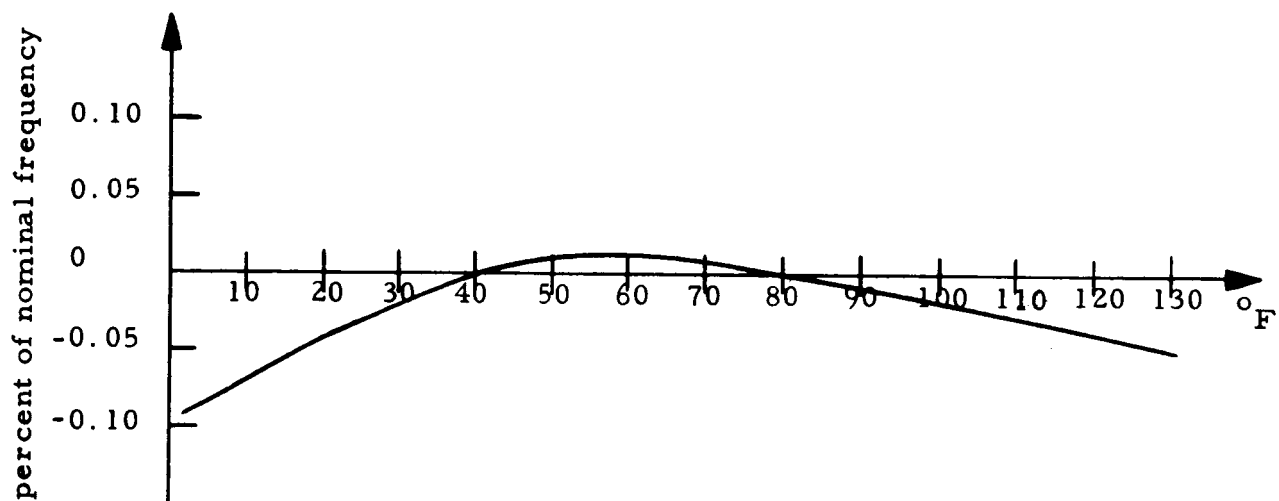


Figure 6. Oscillator characteristic curves.

by a Schmidt Trigger (Q20 and Q21) to drive the binary scaler (Q1 and Q2).

In fulfilling the amplitude symmetry requirement, a tuned power push-pull amplifier develops the sensor drive power. To prevent loading of the binary counter, its output is used only as a gating function to drive the power amplifier and the drive voltage is derived from B+ after attenuation through a thermistor temperature compensation network. Probe sensitivity, however, is a function of drive amplitude and exhibits a peaking effect. Hence the probe operating point is set at the maximum output point where there is the least sensitivity to small changes in probe drive amplitude. To further insure a balanced network, careful selection of matched transistors with temperature, and final circuit trimming is done during the production and test phase. Also, the thermistor network compensates for gross change in probe drive power as a function of temperature. The probe drive signal is then transformer-coupled to the probe in order to avoid passing any d-c current through the probe windings.

The probe output complex waveform presence of an external field is applied to a passive second harmonic filter to extract the field component. Figure 7 shows the bandpass characteristics of the filter.

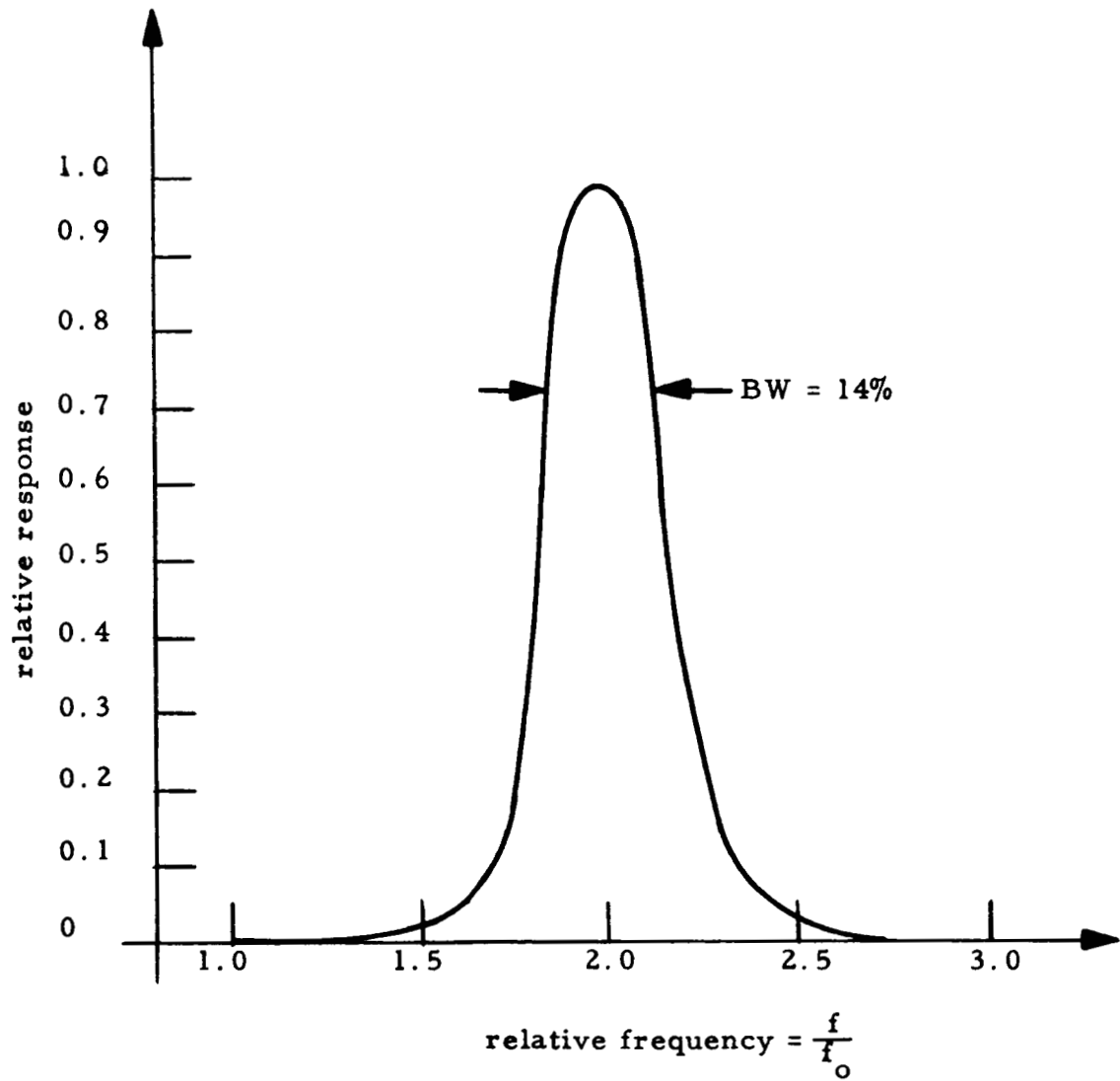
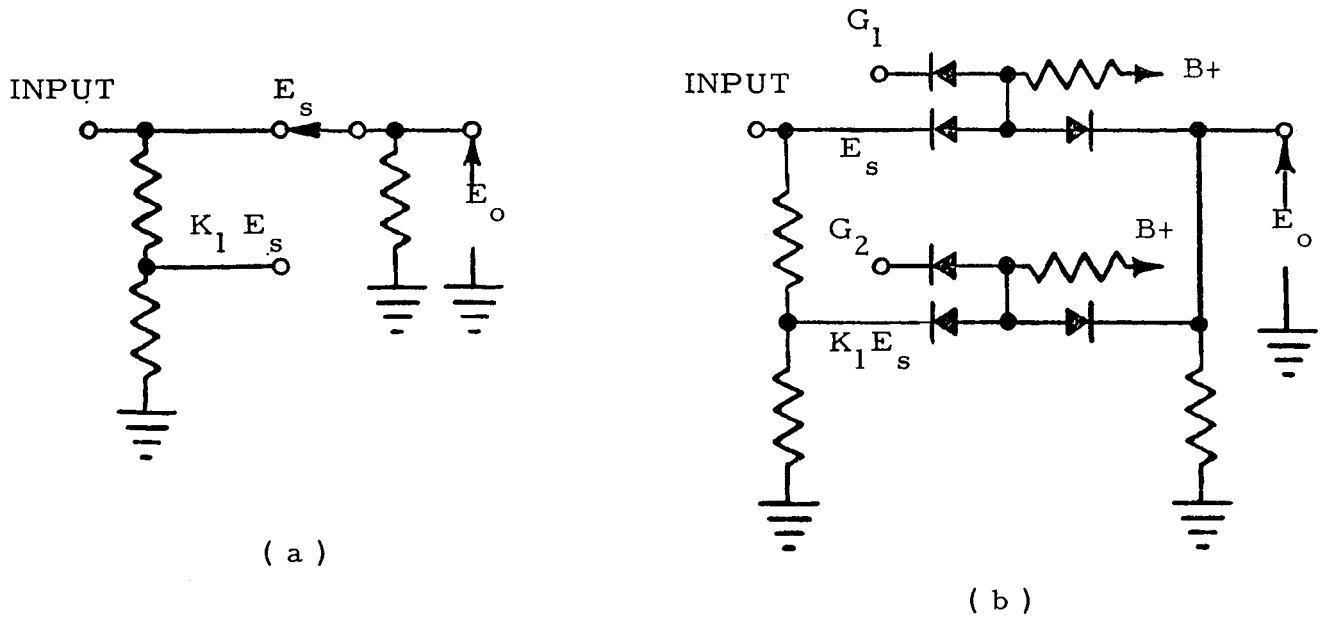


Figure 7. Second harmonic band pass filter characteristics.

The filter (FL 1) alone attenuates the fundamental and third harmonic by about 45 db but the double probe technique further relieves the filtering requirement due to the odd harmonic cancellation effect in the probe secondary winding. Since the filter is not tuneable, the oscillator is tuned to the filter characteristics.

The filtered second harmonic signal is then applied to a diode matrix for scale switching and attenuation. The switching point is arbitrarily selected to be 80% of full scale voltage deflection. This allows a safety margin to prevent the output from exceeding the specified output range due to switching point drift or difference in response time between output and scale switch circuit. Scale switching is accomplished by detecting the absolute magnitude of the field and causing a trigger circuit to switch at a preset level. For two scales of measurement one detector-trigger network is required. The amplitude detector is a diode peak-to-peak detector (CR7 and CR9) and the trigger circuit consists of a Schmidt trigger (Q16 and Q17) that switch on the output of the detector. The trigger output is then used to operate the diode gate.

Figure 8a shows a functional diagram of the scale switching network



TRUTH TABLE

Measurement Range	Scale	S_1	\bar{S}_1	G_1	G_2
-64 γ to + 64 γ	1 - low (most sensitivity)	0	1	1	0
- 320 γ to + 320 γ	2 - high (least sensitivity)	1	0	0	1

(c)

Figure 8. (a) Functional diagram of scale switching network.
(b) Basic circuit.
(c) Field-switch relation.

and Figure 8b shows the basic diode matrix that forms AND-OR logic gates and Figure 8c is the truth table which shows the field-switch relationship. K_n is the attenuation factor and G_n is the gating function where only one G function at a time will equal "one" while the other is "zero". For this condition,

$$G_1 = \bar{S}_1$$

and

$$G_2 = S_1$$

For each axis, the measurement scale is identified by output \bar{A}_1 which is functionally identical to \bar{S}_1 . The output has two distinct d-c levels. State "zero" corresponds to $+0.3v \pm 0.1v$ and state "one" corresponds to $+11.5v \pm 0.5v$. The scale outputs are derived from saturated inverter amplifiers with 12,000 ohm collector load resistor and presented to the DCS for digital storage and transmission.

Although the diodes are temperature dependent, they serve as gating elements only. Also, the measurement is an a-c amplitude modulated system. Hence, only the dynamic impedance of the diodes is of concern and the design is such that diode impedance is negligible compared to the related circuit impedance. After proper attenuation, the signal is amplified by a tuned push-pull amplifier (Q24 and Q25)

driven by a RC paraphase amplifier (Q23) and two stages of RC amplifiers (Q26 and Q27). The tuned push-pull amplifier helps to maintain symmetry and also provides additional filtering. The amplified signal is then presented to the output phase detector network by a transformer coupled emitter follower circuit.

Employing the countdown technique automatically provides a reference signal for phase detection since the basic oscillator operates at the second harmonic frequency. However, because of the numerous tuned circuits involved, an over-all phase control is necessary. This is placed in the reference circuits as opposed to the signal amplifier chain to prevent any signal attenuation. In addition, a passive RLC network is used to obtain temperature stability. Figure 9 shows the basic phase control network consisting of a R, L, and C. (Reference: Vol. 19 MIT Rad Lab Series, page 139.) When

$$2 X_C = X_L,$$

$$\left| E_o \right| = \left| E_i \right|$$

$$\phi = 2 \tan^{-1} \frac{R}{X_L}$$

and

where ϕ is the phase angle between E_o and E_i . Hence, R can control from zero to 180 degrees. Two networks (R104, L1, C39 and R111, L2, C42) are used to give greater phase control. In addition to providing

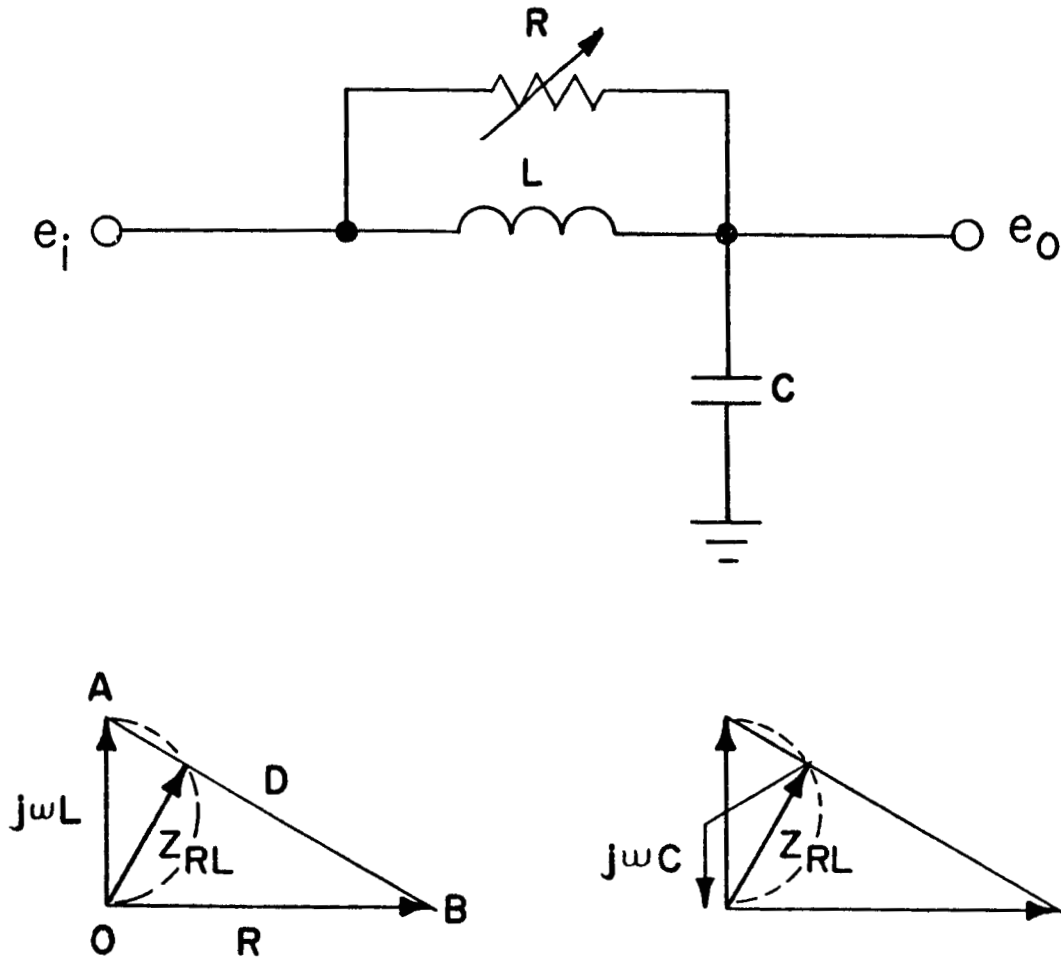


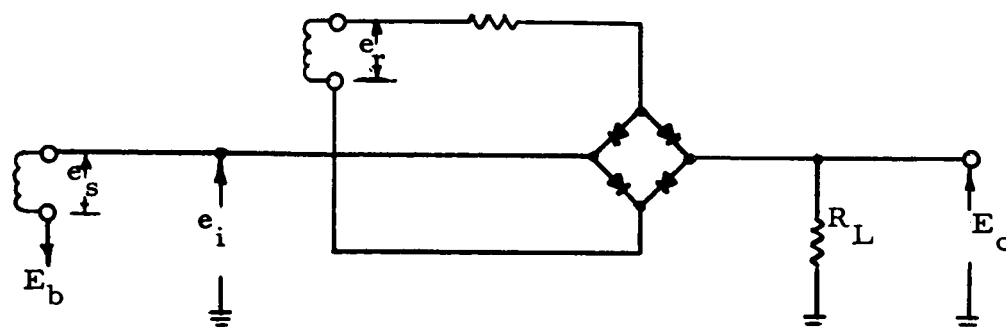
Figure 9. Basic Phase Control Network And Impedance Vector Diagrams.

phase control, the network partly filters the square wave reference signal taken from the oscillator - Schmidt trigger circuit. The reference signal is then amplified and filtered by a tuned amplifier Q33) and transformer (T7) coupled to drive the output phase detector circuit.

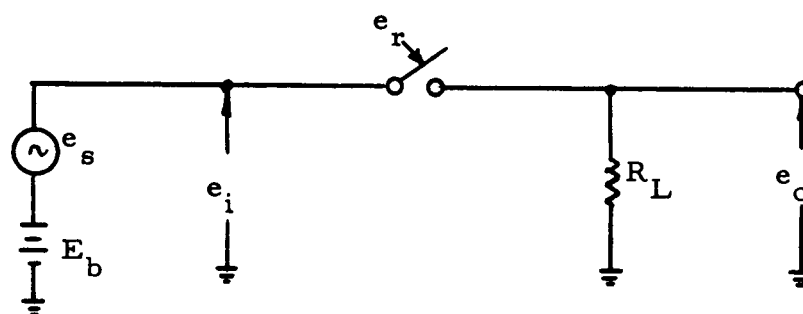
A diode gated, balanced, full wave bridge detector (CR 18, 19, 20 and 21) is used for the output phase detection. This type of detector provides minimum signal attenuation, minimum coupling between signal and reference voltage, and minimum effects by reference signal amplitude change.

Figure 10 shows the basic detector circuit, functional diagram, and relative waveforms. The diode bridge gate acts as a SPST switch which is driven by the reference signal at the second harmonic frequency. The relative phase between the reference and field signal is adjusted such that, ideally, the detected output will be a half wave rectified sinusoid riding about the bias level E_b . The detected output is then filtered by a low pass filter (C46) and limits the response of the unit with one second time constant. The data output (E_o) is then characterized by,

$$E_o = E_b + KH \cos \theta$$



(a)



(b)

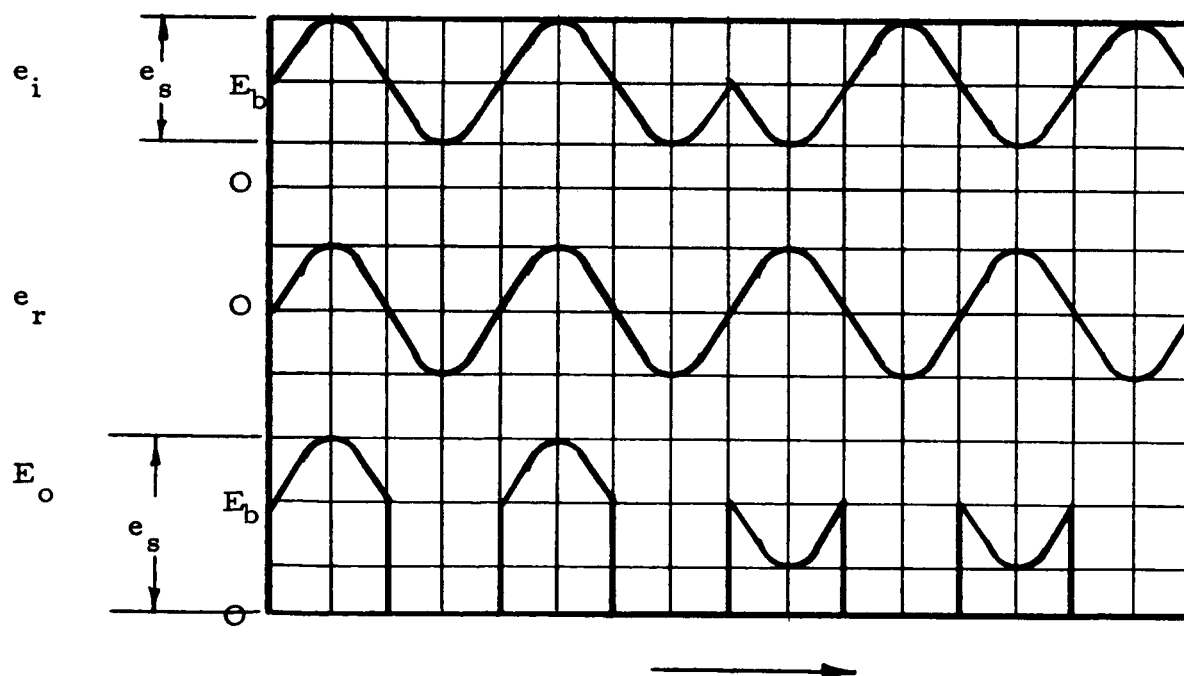


Figure 10. (a) Basic phase detector circuit.
(b) Functional diagram.
(c) Relative waveforms.

where K = constant
 H = external field being measured
 θ = phase angle between reference and signal voltage
 E_b = zero field bias voltage

The final data output signal to the DCS is a d-c voltage biased at +3.5 volts for zero field and plus or minus 2.5 volts full scale deviation from the bias level for plus or minus field variations, respectively. Scales one and two, however, are automatically switched at plus or minus 2 volts deflection to provide safety margins as discussed previously. The output zero field bias voltage is developed by attenuating the supply voltage and the stability is therefore relative to supply regulation ($\pm 0.2\%$). In the output buffer stage (Q34) is a PNP-NPN emitter follower which cancels the d-c drift inherently occurring in base-emitter junction. Between 0°F and $+125^\circ\text{F}$ stability is within 15 mv.

Figure 11 shows the schematic diagram of the in-flight calibrate and null field circuit. The in-flight calibration functions upon command from the DCS is performed to check the operation of the unit. A calibrated field of about 32 gamma is generated by passing current through the probe auxiliary windings to determine scale one sensitivity. The circuit is designed to reset itself to normal operation upon command from the DCS.

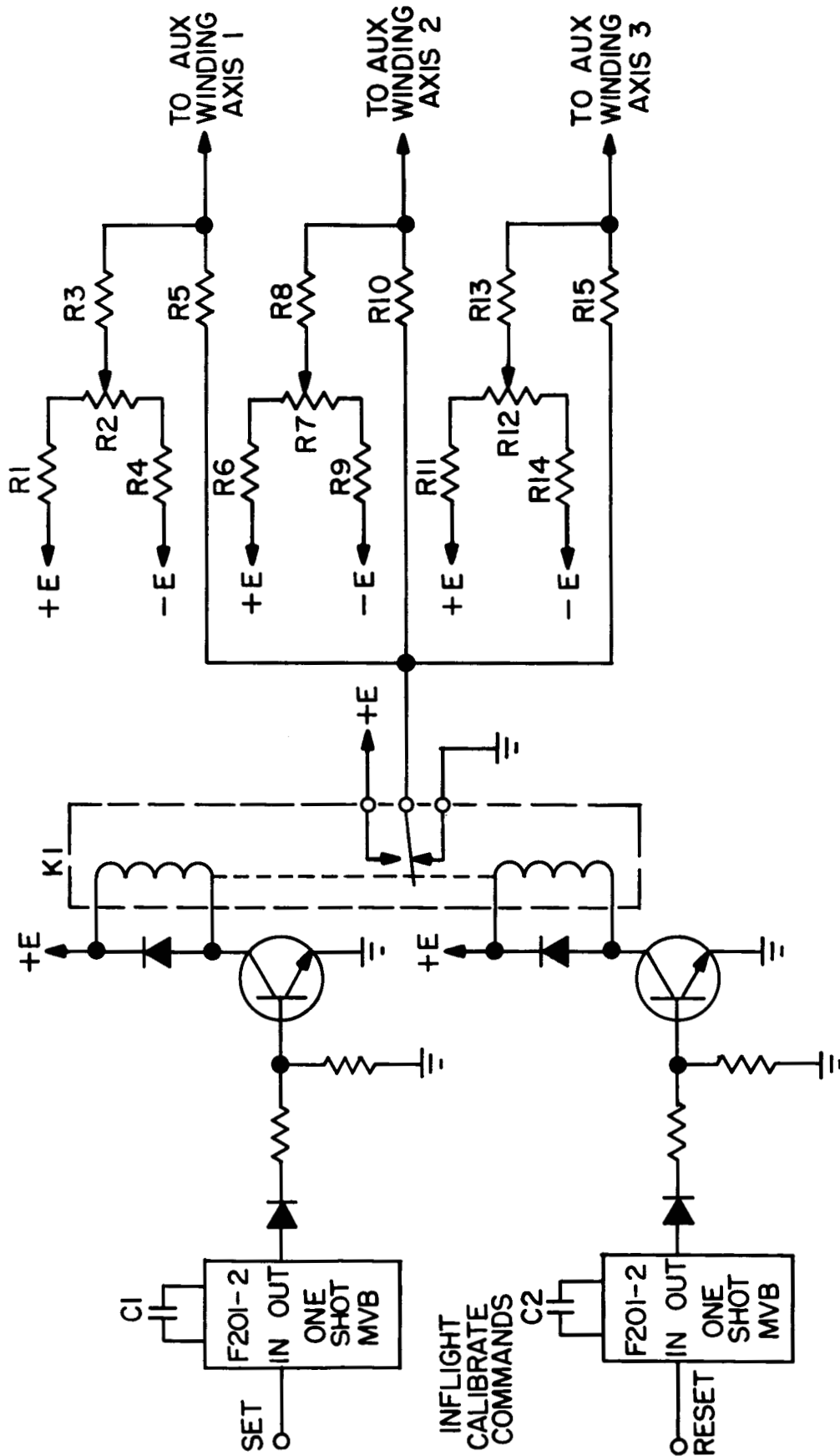


Figure 11. In-Flight Calibrate And Null Field Circuit Schematic

The waveform and relation between command signal and readout period is shown in Figure 12.

The calibrate command signal triggers a one-shot multivibrator which drives the relay driver transistor (Q1) on for 50 milliseconds to energize the latching relay (K1) to the ON position. Resistor (R5, 10, and 15) are selected for the proper calibrate current to the auxiliary winding. The reset function is carried out by a similar circuit consisting of a one-shot multivibrator and a relay driver transistor (Q2) which energizes the reset coil of the relay (K1).

The null field circuit is a static adjustment to cancel the magnetic moment of the payload. The circuit consists of R1, 2, 3 and 4. Potentiometer R2 is for current control, R1 and R4 are divider pads, and R3 is the current limiting and impedance matching resistance.

Power Supply: Figure 13 shows the power supply schematic diagram. The primary purpose of the unit is to accept 100v $\pm 10\%$ peak-to-peak square wave at 2400 cps and convert it to +12.00v d-c $\pm 0.2\%$ over the temperature range from 0°F to +150°C with load capacity of 300 milliamperes.

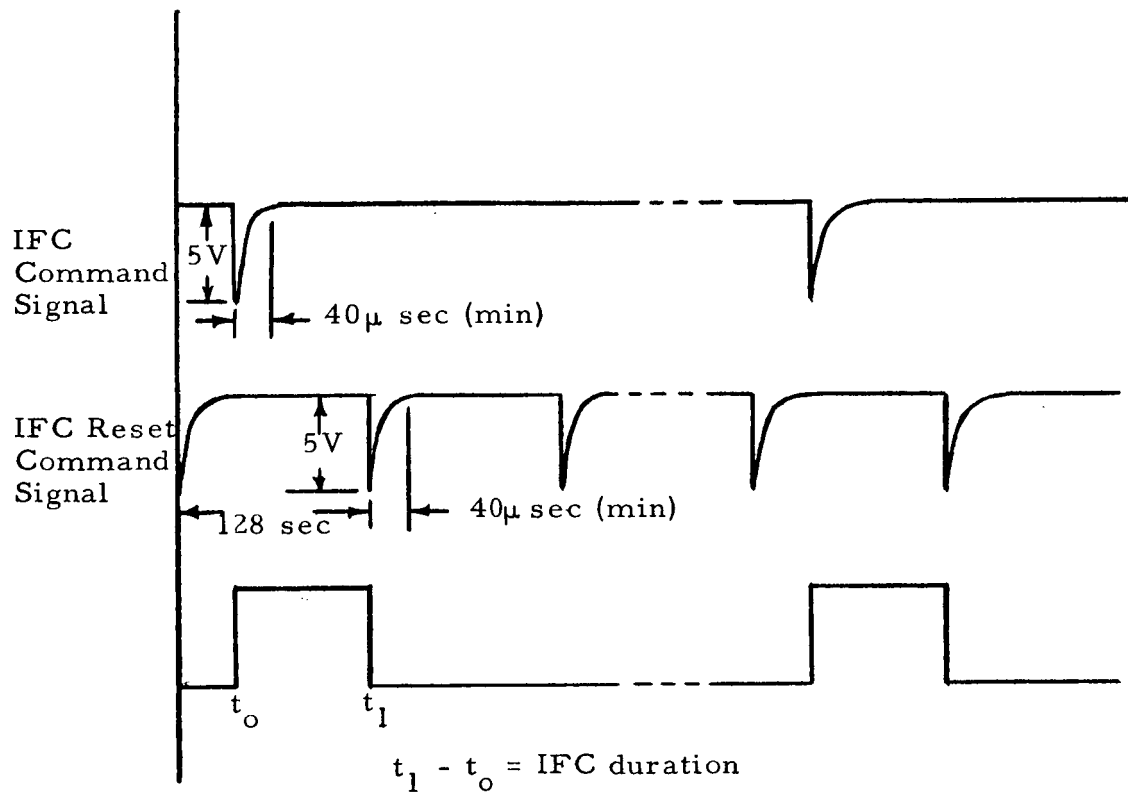


Figure 12. In-flight calibration (IFC) command signal.

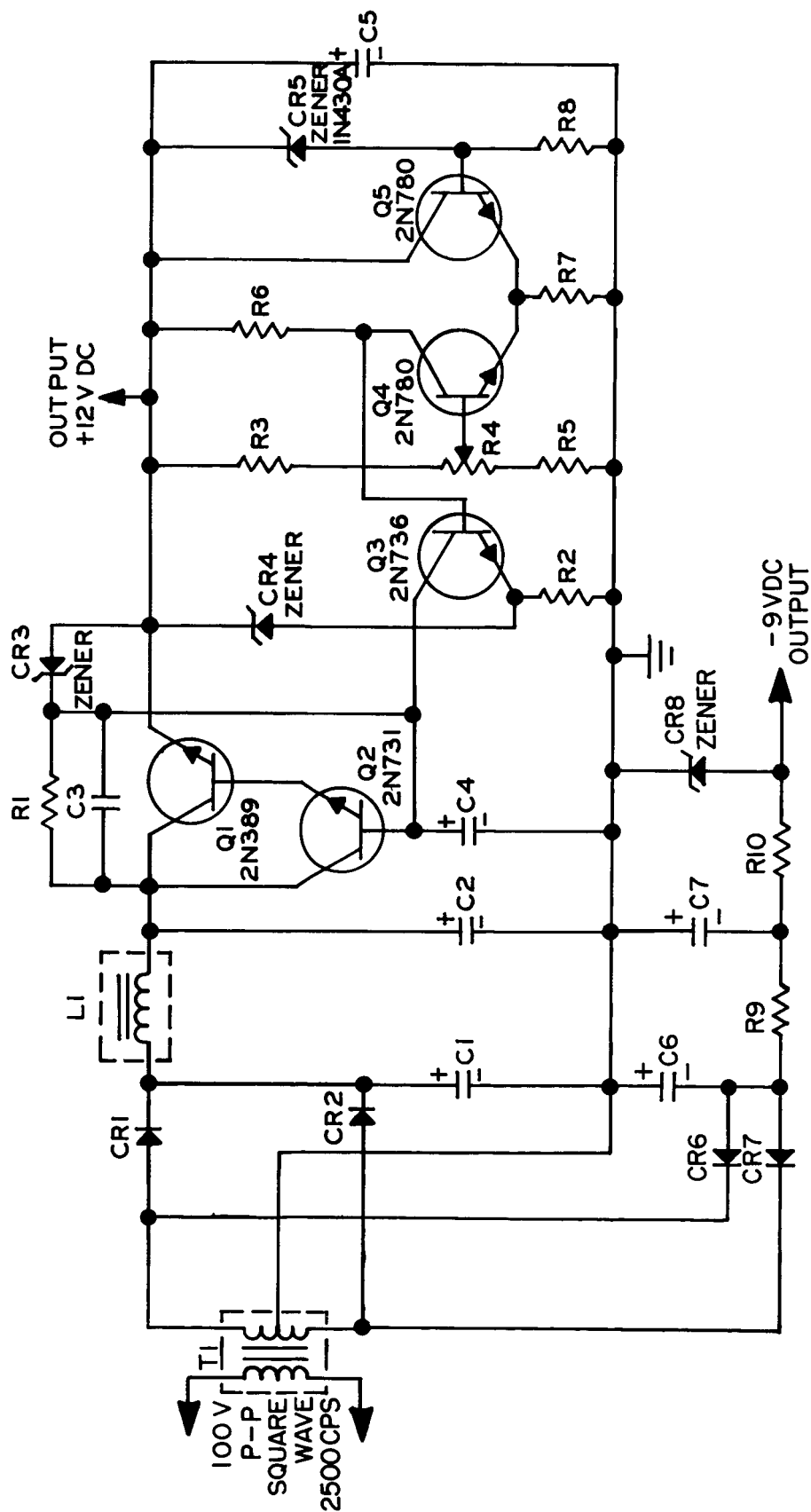


Figure 13. Regulated Power Supply +12 And -9 V d-c

The design standard set up at the result of this compromise were as follows:

1. Use standard JPL housing with required modification. Material of housing is to be Magnesium.
2. Fork-type terminals to be employed.
3. One lead wire per terminal.
4. Modules mounted on board with RTV 891 potting compound with leads from modules extending parallel to printed circuit board.
5. Large Durmica type capacitors to be mounted on their sides flush to board and spot potted with RTV 891.
6. Adhere to JPL Spec. S20016, "General Specification, Workmanship Requirements for Electronic Equipment".

Use of one lead per terminal could not be adhered to throughout because of the density of components. Terminals were used as feed through devices in getting continuity for circuitry on one side of the board to the other. Plated through holes were not used as a feed through because upon insertion of the terminal the plating on the inside of plated through hole could be damaged.

The only conductor lines on the back of the board were B+ and ground.

All other conductor lines appeared on the component side of the board. This decision entailed the use of many jumper wires on the component side of the board, the back side of the board being bonded flush to the web with Eccobond 55 making rework impossible.

The transformers were held by screws which went through the board and attached to the web, thus aiding the board attachment. The transformers were shielded with conetic foil to minimize cross talk and noise pick up from adjacent transformers. Transformers were also staggered so no two transformers were in line in order to eliminate field alignment.

The high energy probe transformer was isolated as much as possible to minimize secondary harmonics pick up from other transformers and circuitry.

Trimpot adjustments and test jacks were situated near the periphery of the board for ease of adjustment during check out and calibration.

Splicing and the shielding of wire was according to JPL Specifications 20500 and 20501.

The coating material used on the board was Uralane 241. This material is easy to remove when the printed circuit board requires re-work and it also behaves like a fluxing agent.

Marshall Laboratories standard F-line Modules were employed wherever they could be utilized. In the use of these modules the package of the electronics was achieved. If the components within these modules were mounted on the printed circuit board, packaging of the electronics into the allocated volume would not have been attained.

The concept of having a continuous full web across the housing was justified when the unit passed environmental testing. The web gave the housing good rigidity during any axis of vibration.

The Mariner "R" Triaxial Fluxgate Magnetometer weighed 4 pounds, minus the sensor unit, the physical outline dimensions being $6 \frac{1}{8} \times 6 \times 3 \frac{3}{4}$. The unit qualified in all phases of environmental testing performed by JPL.

Figure 14 shows a photo of the final flight electronics unit and Figure 15 shows the flight sensor unit.

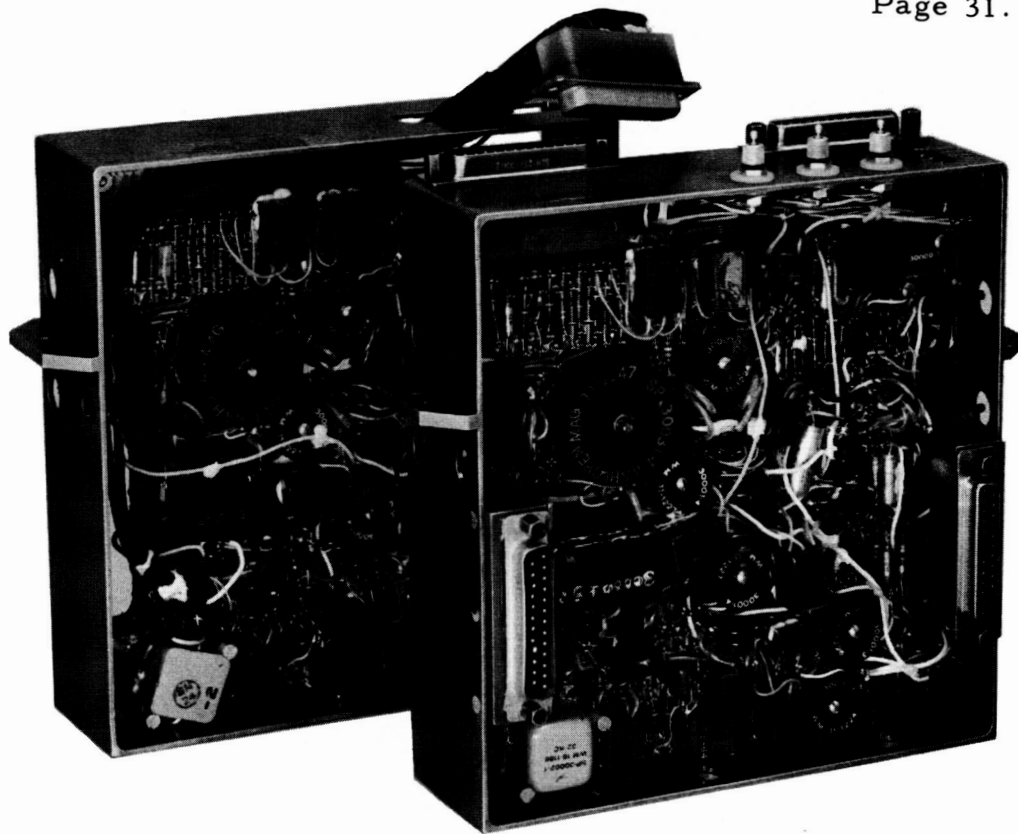


Figure 14. Final Flight Electronics Unit

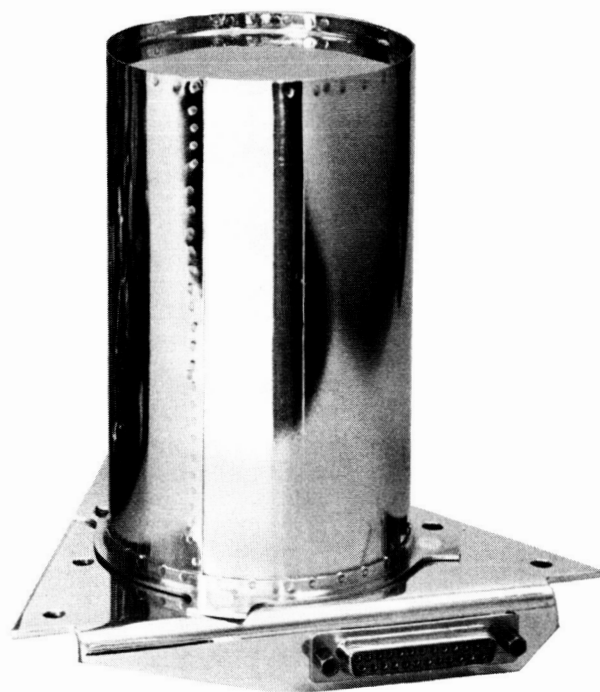


Figure 15. Final Flight Sensor Unit

Special Purpose Equipment.

Three major special purpose equipment are used to assist in successfully developing the magnetometer unit. These are the Cylindrical Fluxtank, Spherical Fluxtank, and Checkout Suitcase and Adapter Unit.

Development of a magnetometer to measure planetary and inter-planetary magnetic fields (several gamma) requires a "field free" test volume to shield against earth's magnetic field (about 60,000 gamma) and man-made disturbances. Uniform controlled and calibrated fields are then generated to test and calibrate the magnetometer. Such requirements led to the design of the fluxtanks.

The checkout suitcase, along with the adapter unit, is designed to test the performance of the magnetometer in a go-no-go manner.

Cylindrical Fluxtank: The Cylindrical Fluxtank (Model ML 102-1) is limited to testing monoaxial magnetometers. But, several tanks will allow a parallel effort in pre-testing and calibrating individual sections of a triaxial instrument. The tank is comparatively small, easy to handle and operate, and has proven to be very versatile. The tank is composed of eight concentric cylinders of steel, mu-metal and copper.

The outer cylinder is made of steel which provides external structural rigidity as well as magnetic shielding with relatively high saturation characteristics. The remaining cylinders are alternately of copper and mu-metal. The mu-metal cylinders provide most of the field attenuation with high permeability characteristics, whereas electric field shielding is provided by the copper cylinders.

The lid assembly is designed to completely enclose the cylinder, providing minimum magnetic leakage with maximum ease of handling. Such requirements led to a "vault door" type design, where the lids were matched to the cylinders during fabrication for slip fit.

A solenoidal coil, five inches in diameter and 25.5 inches long, with two identical windings, is fitted into the cylinder. One winding provides a magnetic field to null the leakage residual field and any permanent field that may have resulted after manufacture. Measurements showed about 200 to 300 gamma residual field. The second winding provides calibrated magnetic field. A pair of small rectangular cross trim coil may be used to null any excessive cross field that may be present.

The sensor fixture inserts into the coil form with fixed connectors

providing electrical signal continuity. The fixture is then easily removed from the tank and is easily modified to accomodate various sensors at minimum cost. The sensor may be rotated through 180 degrees in one axis without removing the fixture to determine zero field offset or probe perm. The null cross field is placed in line with the direction of rotation to reduce mechanical tolerance requirement. Testing in the other axes of a triaxial sensor requires remounting and reorientation. Figure 16 shows the fluxtank internal assemblies.

The probe and field coil cables are united through the cylinders to minimum field leakage, and terminate at a convenient 25 pin female connector. The overall dimensions of the tank are 30 inches in height by 12-1/2 inches in diameter. Figure 17 shows the cylindrical fluxtank.

Stable calibrated currents are supplied by the associated electronic control unit to the solenoid windings in the fluxtank for generation of specific magnetic fields. The heart of the electronic control unit is a manually operated binary-to-analog linear staircase generator with constant source impedance. Each generator section is arranged in decade fashion and the output currents are summed at the solenoid coil.

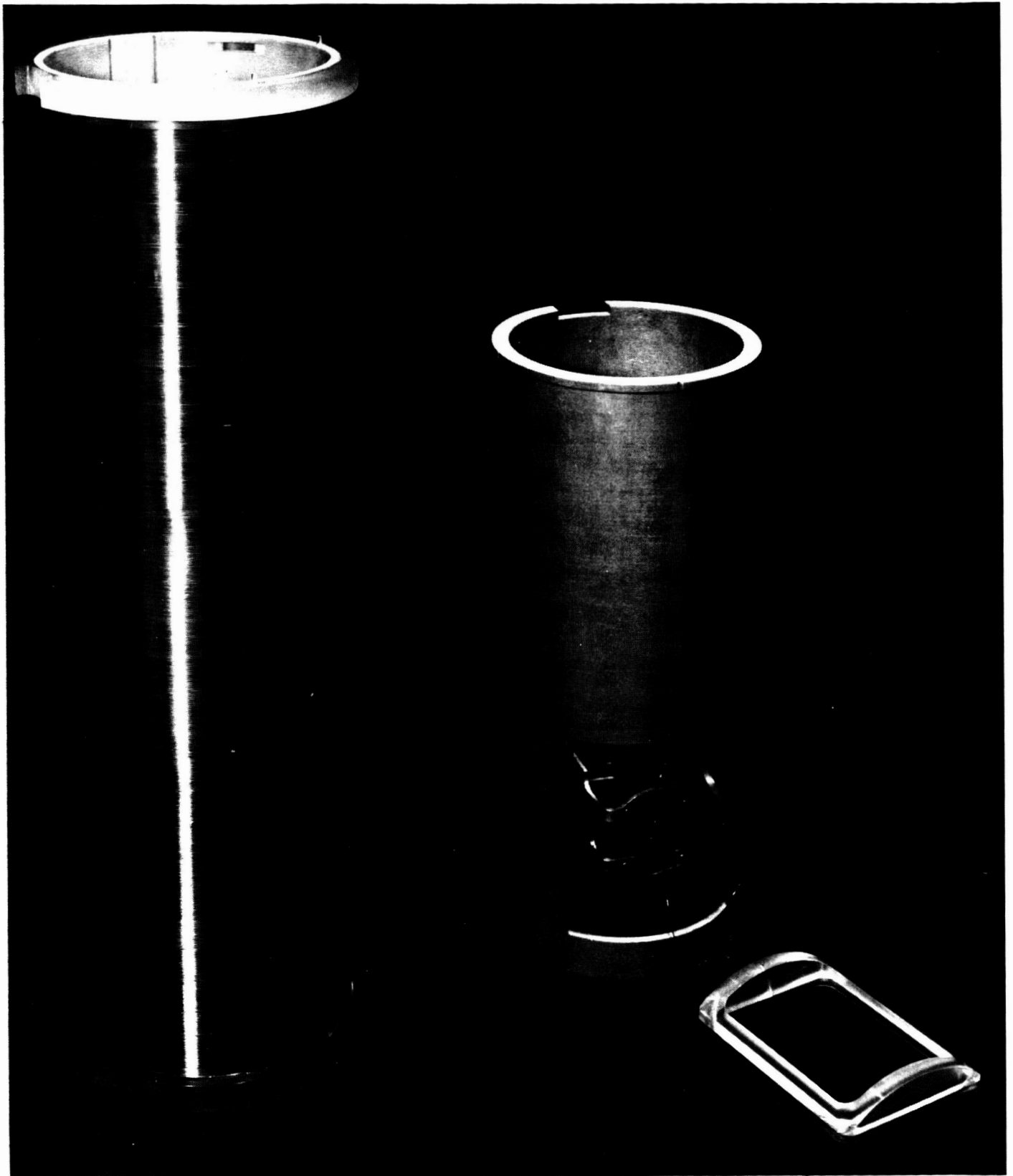


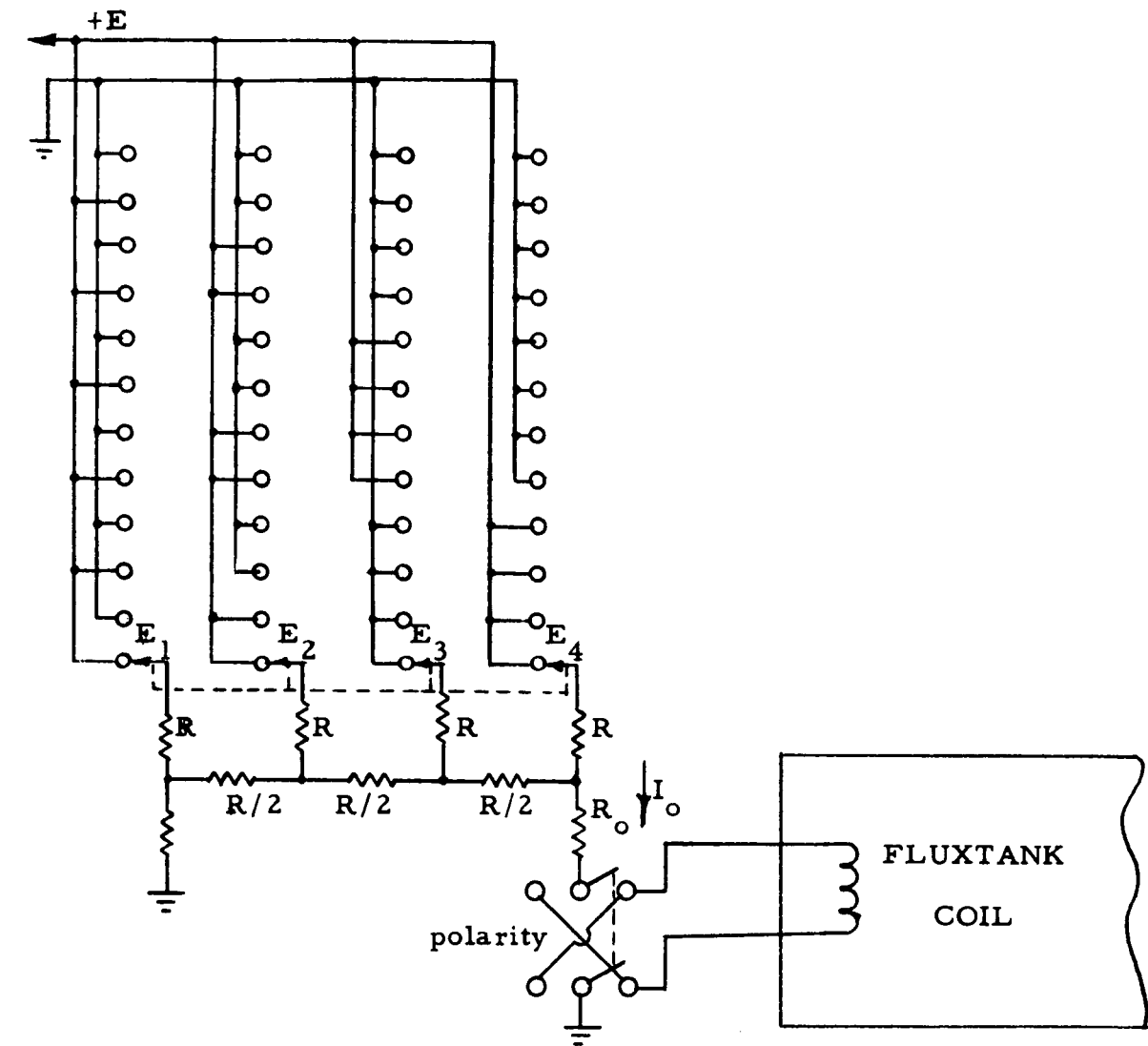
Figure 16. Cylindrical Fluxtank Internal Assemblies



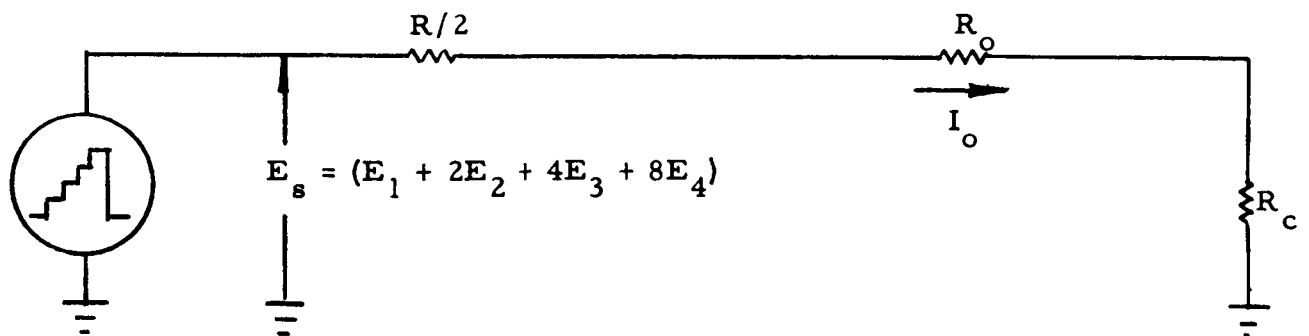
Figure 17. Cylindrical Fluxtank, Model 102-1

The basic current generator is shown in Figure 18a. Each switch deck represents a binary bit where $S_1 A$ is the least significant bit. The voltages E_1 through E_4 will either be $+E$ or zero (binary code one or zero, respectively). Resistor R_o is adjusted for the proper I_o during initial calibration of the unit. S_2 is used to reverse the direction of current through the coil, thereby reversing the direction of the magnetic field. The equivalent circuit is derived by successively applying Thevenin's transformation with the result shown in Figure 18b. It is noted that the network has a constant source impedance ($R/2$). Linearity is therefore a function of resistor tolerance; $\pm 0.1\%$. The stability of the field is seen to be a function of the power supply voltage ($+E$) which is $\pm 0.1\%$. With R_c (coil resistance) much less than R_o , each generator section output can be applied to the coil and the currents will be additive. Null fields up to 1000 gamma are available with one gamma/step control and five gamma continuously variable vernier control. Calibration fields up to one gauss are available with one gamma/step control, and five gamma continuously variable vernier control.

Spherical Fluxtank: The Spherical Fluxtank (ML103-2) is designed to allow testing of the triaxial magnetometer in its complete operational state for parameters such as d-c field crosstalk and inter-axis a-c



(a)



(b)

Figure 18 (a) Stairstep generator circuit
(b) Equivalent circuit

modulation. The tank is composed of six concentric spheres of steel, mu-metal and copper. The outer shell is of steel to provide external structural rigidity as well as magnetic shielding with relatively high saturation characteristics. The remaining spheres are alternately of mu-metal and copper. Three mu-metal spheres provide most of the field attenuation with high permeability characteristics, whereas electric field shielding is provided by two copper spheres. Measurements have shown that the residual field is about 100 to 200 gamma, with approximately one gamma per inch gradient within a six inch diameter test volume at the center of the sphere. The outside and inside diameters are approximately 48 and 43 inches, respectively. Access to the interior chamber is provided by separating the hemispheres with a hoist as shown in Figure 19. Both halves of the sphere are designed to completely enclose the interior for minimum magnetic leakage but with maximum ease of handling. This is accomplished by careful design and close tolerance control during manufacturing.

A 30 inch diameter triaxial Helmholtz-Gauguin coil array is used to generate magnetic fields. Each axis has two windings. One winding is used to null the residual field and any permanent field that may result after manufacture, and the other winding provides calibrated magnetic

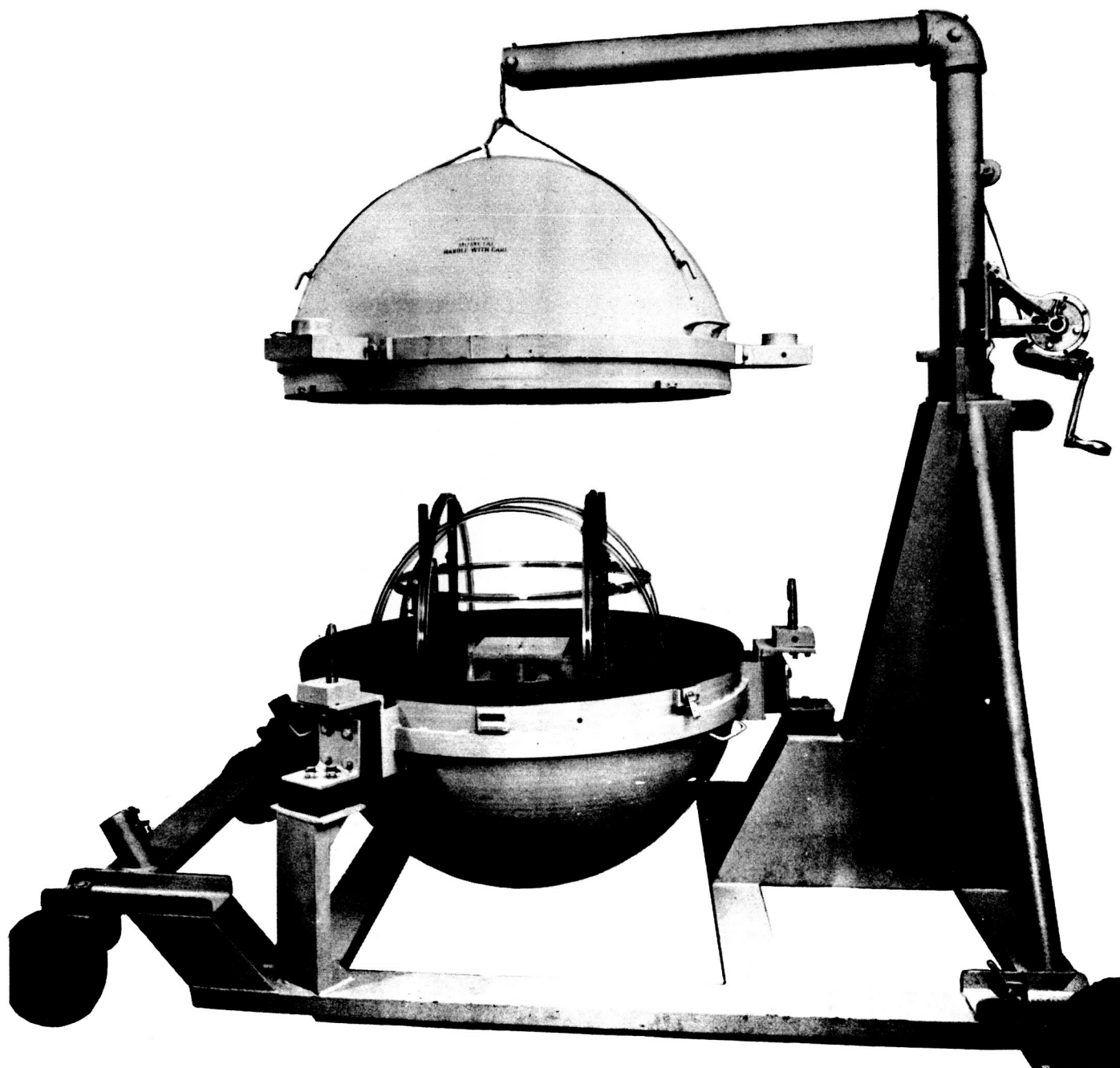


Figure 19. Spherical Fluxtank, Model ML 103-2

fields. The coil forms are made of non-metallic material and designed to provide two true Helmholtz-Gaugain coils per axis as shown in Figure 20. That is,

$$\frac{A_1}{D_1} = \frac{a_1}{d_1}$$

The design equations per coil are,

$$x = \pm 0.11a$$

$$y = \pm 0.14a$$

for a uniform region; a current

$$i = 1.1121a \text{ amperes}$$

would produce a field of one gauss at the center. For simplicity, each coil is wound with 25 turns and has a nominal coil constant of 15 micro-amperes per gamma.

Figure 21 shows the functional diagram of the field control unit (ML 112-2). The field generator sections are similar in design to the cylindrical fluxtank electronics. For each axis, null field in steps of 100

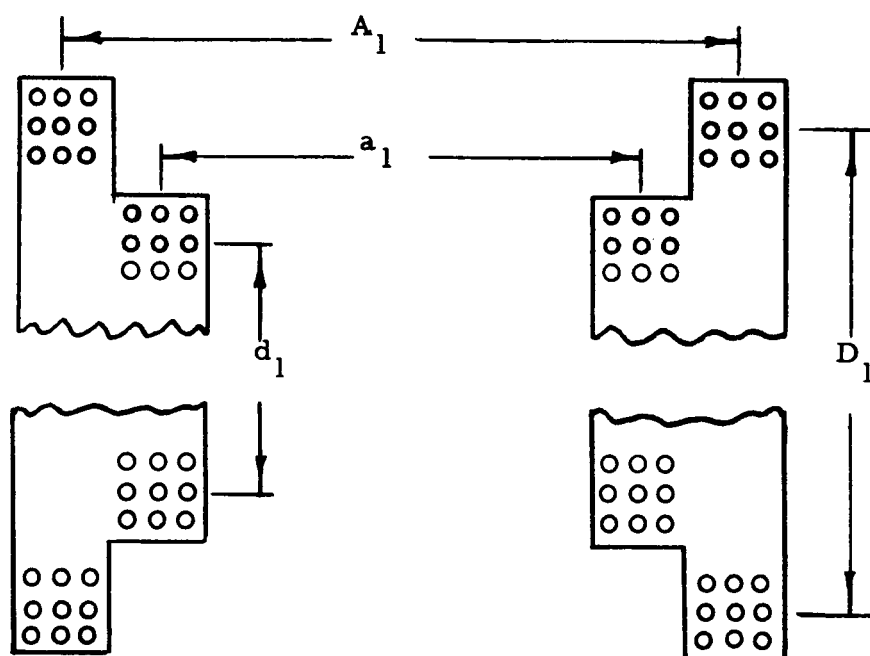


Figure 20. Dual Helmholtz coil form.

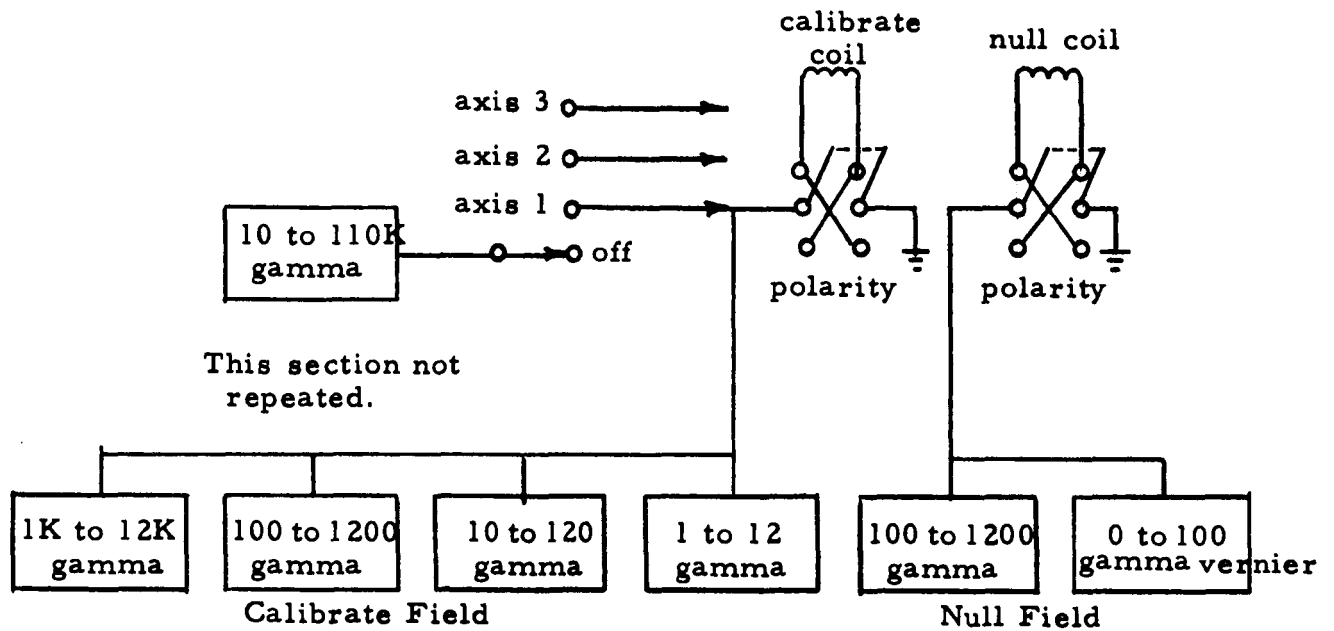


Figure 21. Functional diagram of spherical fluxtank control unit for one axis. All axes are identical.

gamma up to 1,200 gamma is available with 100 gamma continuously variable vernier control and calibrate field in steps of one gamma up to 12,000 gamma can be generated. High field in steps of 10,000 gamma up to 110,000 gamma can be generated in any one axis at a time by manual selection. The stability of the field is a function of the power supply voltage stability which is $\pm 0.05\%$. The accuracy of the field is a function of the accuracy of current limiting resistors which is $\pm 0.05\%$.

To locate the magnetometer sensor on center, the sensor mounting assembly is designed to provide lateral and vertical movement of about six inches. Rotation of the probe through 180 degrees, to determine zero field offset, is also provided. Each function is controlled externally through flexible cable as seen in Figure 22.

Checkout Suitcase And Adapter Unit: The checkout suitcase for the magnetometer is a portable test set to be used during environmental, bench, and payload manner. It was developed for the Mariner A program. The suitcase contains circuits for:

- a. generating d-c magnetic field for null and calibration,
- b. generating a-c magnetic field to excite the spectrum analyzer,
- c. monitoring pertinent output signals,



Figure 22. Lower Hemisphere of Spherical Fluxtank,
Helmholtz Coil, Sensor Fixture and Sensor.

- d. simulating command signals, and
- e. providing d-c power.

To utilize the suitcase for this program, it was necessary to design and build an adapter unit. The adapter unit provides the necessary functions which specifically meets the requirements of the Mariner R magnetometer which cannot be provided by the Mariner A checkout suitcase without modification. The unit provides the following functions:

1. shapes and selects in-flight calibrate command signals.
2. shorts the secondary of the probe to check electronic zero.
3. spot checks the output sensitivity of each of the two ranges.

The adapter unit schematic diagram is shown in Figure 23. See Test Procedure, S40064, for operation of suitcase and adapter unit. With the pulse selector on the appropriate position, the positive pulse formed by depressing the push button on the suitcase is converted to a fast negative five volt pulse which can be switched to set or reset the IFC relay circuit.

The shorting switch provides a means of checking the electronic zero and also providing a means of checking the operation when the probe is in such a high ambient fluctuating field that the null controls on the

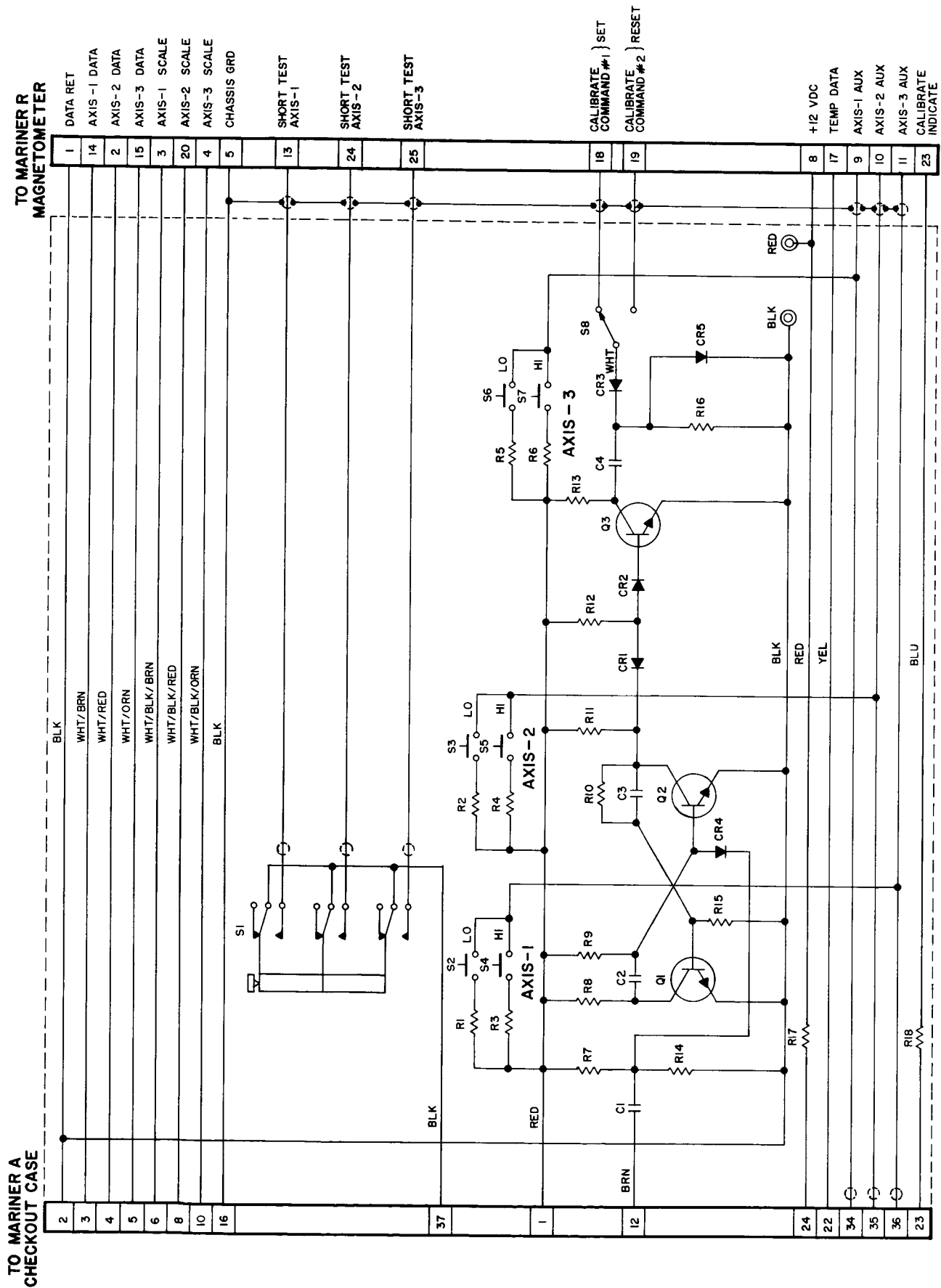


Figure 23. Checkout Adapter Unit Schematic Diagram.

suitcase cannot bring the unit into its high sensitivity range.

The "lo" and "hi" push buttons when activated will produce a constant current of 15 and 150 microamperes which corresponds to 30 gamma and 300 gamma, respectively. They provide a one-spot, repeatable calibration point on each of the two scale.

A block diagram of the suitcase is shown in Figure 24. To provide known magnetic fields for checkout, the system utilizes the auxiliary windings within the sensor. Since the coil constant K , $(H-KI)$ is known to be about 0.5 microamperes per gamma, the effect of the earth's field on the sensor may be effectively cancelled by passing a controlled, constant, "null" current through these auxiliary coil. The effect of this field on the magnetometer is displayed by panel meters which monitor the magnetometer data and scale outputs voltages. The following controls are not used but will be described. The calibrate field generators, operating from independent power supplies, add to, or subtract from the current generated by the null field generators and simulate a desired change in magnetic field, H . To provide one-spot, repeatable calibration points, push-button switches are employed to switch in a known constant current; i. e.; a constant field, one field for each range.

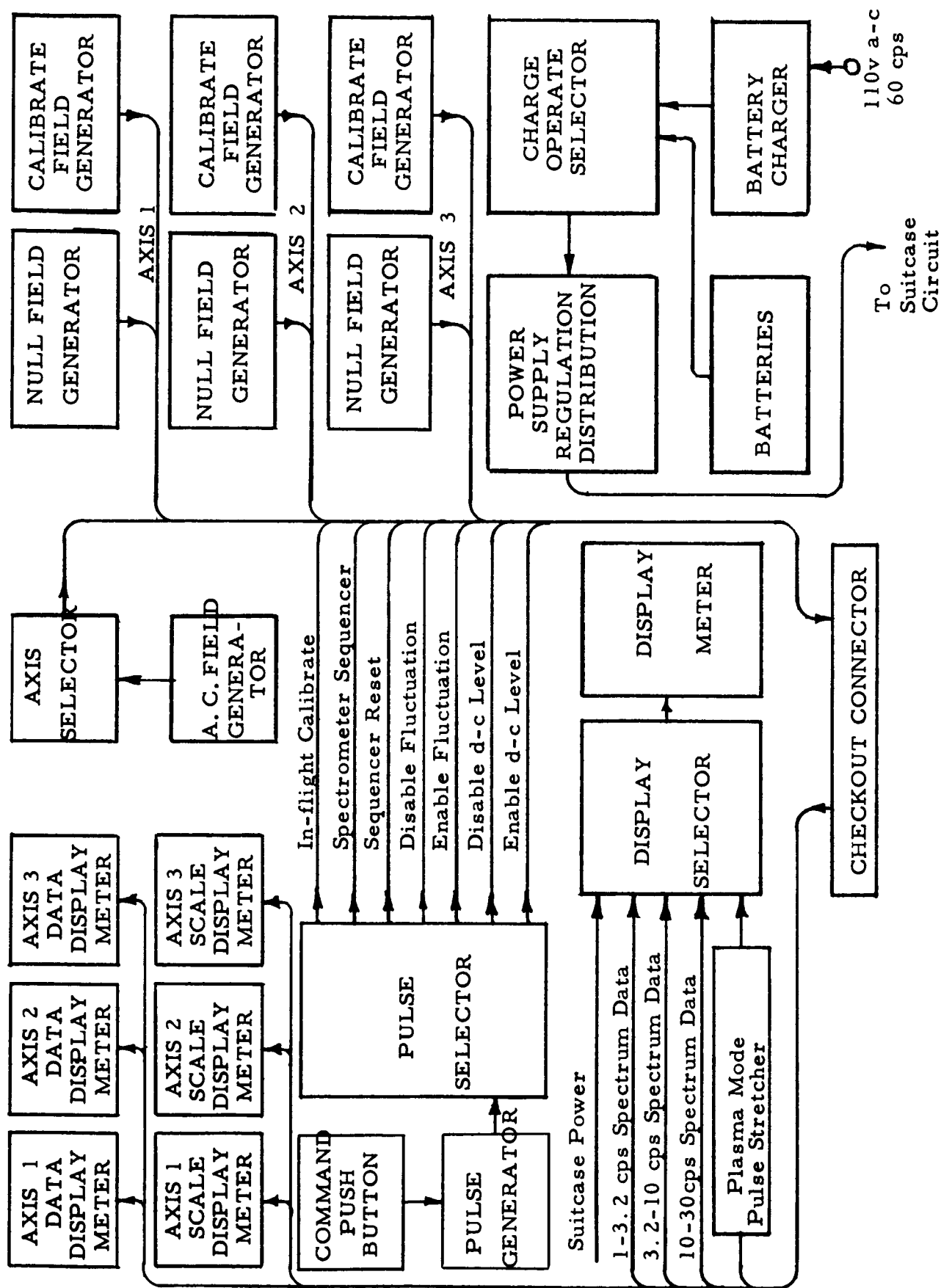


Figure 24. Block diagram of Suitcase Checkout System.

Primary suitcase d-c power is provided by rechargeable batteries, an internal series regulator is used to develop +12.00 volts. A self-contained battery charger will fully restore the batteries in less than 12 hours by using a taper charge technique. Primary magnetometer a-c power is not provided by the suitcase. Mercury batteries are employed to supply a stable, one volt reference to the calibrate field generators with an expected life of over one year.

S40064 (Appendix B) describes the test procedure of the suitcase unit and adapter unit.

TESTING AND CALIBRATION

After each of the sub-units has been assembled, they undergo two phases of electrical testing. The first phase involves determination of selected values and adjusting final variables such as potentiometers. For phase two, a pre-calibration test as a function of temperature is performed. Final unit calibration is then performed with the magnetometer unit assembled in its final state. If time permits, the unit is operated continuously for about two weeks. Test procedures for each sub-unit have been prepared and are presented in the Appendices.

Pre-Calibration Adjustments.

S40079 (Appendix B) describes the initial bench checkout procedure for the fluxgate magnetometer sub-unit. The procedure basically outlines the process of tuning all band pass LC networks, adjusting gain and scale switching points, determining temperature compensating network, and performing preliminary tests to measure zero field offset, sensor perm, etc.

S40079 (Appendix B) also describes the checkout and calibration of the power supply unit. The performance of the regulator is determined with regard to load regulation under temperature and the ground command relay networks are operated to check their operation.

Final Calibration: S40079 (Appendix B) describes the final calibration procedure for the magnetometer unit as a complete system. Final calibration data for the magnetometer and in-flight calibrator, are obtained at this time. The Spherical Fluxtank is utilized for triaxial operation with the electronics subjected to varying ambient temperature. Typical test results are reported in Appendix C.

SUMMARY

All of the primary objectives set forth in developing the Mariner A Magnetometer Unit were achieved. Some specifications were exceeded while others were relaxed. The final performance of the magnetometer electronics unit is summarized in the following list of specifications.

1. Input power: 100v \pm 10% peak-to-peak, square wave, 2400 cps,
at 100 milliamperes, peak-to-peak (6 watts).
2. Magnetic field data output: Analog voltage between +1v corresponds to the negative field scale limit, +3.5v corresponds to zero field, and +6v corresponds to the positive field scale limit. The output response has a one-second time constant. Output impedance is less than 1,000 ohms from an emitter follower circuit. Linearity is better than \pm 5% of full scale. Noise level is less than than one gamma.
3. Zero field output bias voltage stability: \pm 15 millivolts.
4. Measurement range: \pm 64 gamma for scale one, and \pm 320 gamma for scale two. The range of measurement is automatically switched by the electronics.

5. Operating temperature range: 0°F to $+125^{\circ}\text{F}$. Useful to 150°F .
6. Zero field offset temperature stability: ± 5 gamma.
7. Stability with high field: 5 gamma, after applying 50,000 gamma.
8. Weight: Electronics - 4.1 lbs.

Sensor - 0.67 lbs.

9. Dimensions: Electronic - $6-1/8 \times 6 \times 3-3/4$

Housed Sensor - 5 x 3 diameter unit on $6 \times 3-1/2$ bracket

10. In-flight calibration: DCS command

32 gamma

Due to the limited time allowed for extensive circuit development, some circuits need improvement. This is being done in modifying the magnetometer for Surveyor. Accurate measurement of magnetic field below one gamma is limited by the present laboratory setup. Extensive tests have been performed on the electronics and room temperature tests on the sensor. Since the sensor will encounter space environment, the question still remains as to the performance of the sensor when subjected to $+130^{\circ}\text{C}$. Further investigation in this area is recommended.

ML/TN - 2000.47
Page 54.

APPENDIX A

SENSOR ANALYSIS

In order to facilitate the mathematical analysis of the probe, the following assumptions are made to idealize the core characteristics.

1. Hysteresis is negligible.
2. Flux density is directly proportional to field intensity before saturation.
3. dB/dH is zero beyond saturation.

It is also helpful to introduce the notion of relating the external field H through the probe to an equivalent current such that,

$$\frac{H}{i} = \frac{0.4\pi N}{\ell} \frac{\text{oersteds}}{\text{amperes}}$$

where

N = number of turns

ℓ = length of core in cm.

Figure 25. shows the flux-current relation. The total driving current is,

$$\begin{aligned} i &= I + I_o \\ &= I_m \sin \omega t + I_o \end{aligned}$$

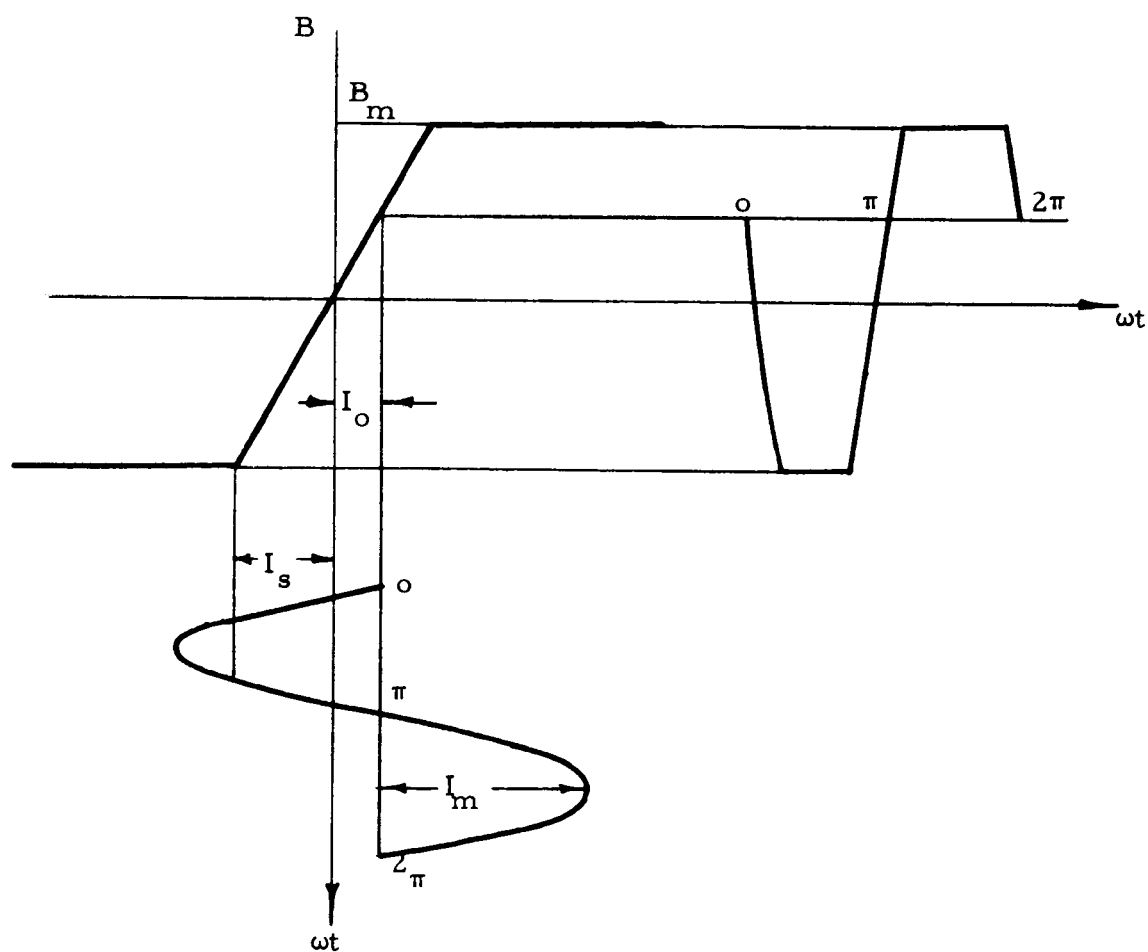


Figure 25. Flux-Current Relation.

where I_m = peak amplitude of the driving current
 I_o = equivalent current related to H.

Obviously, the resultant field waveform contains strong even and odd harmonics of ω because of the unsymmetry. If I_o is zero, the waveform would be symmetrical and contain only odd harmonics. This leads us to suspect that the H function would be contained in the even harmonics and, the second harmonic usually being of the greatest magnitude, the solution is narrowed to determining the second harmonic content of the flux waveform by Fourier analysis.

The general method would be to evaluate

$$B_2(t) = a_2 \sin 2\omega t + b_2 \cos 2\omega t$$

where

$$a_2 = \frac{1}{\pi} \int_0^{2\pi} B(t) \sin 2\omega t \, d\omega t$$

$$b_2 = \frac{1}{\pi} \int_0^{2\pi} B(t) \cos 2\omega t \, d\omega t$$

Since the information is to be detected in the secondary winding as a voltage,

$$e_o = -NA \frac{dB_2(t)}{dt} \times 10^{-8} \text{ volts.}$$

A complete analysis is presented by U. S. NOL (NOLR 830, Design and Development of the Magnetic Airborne Detector, 3 January 1950) the results of which is,

$$e_o = \sqrt{2} S_2 H \cos 2\omega t \text{ volts}$$

where

S_2 = RMS second harmonic output coefficient

$$= \frac{8\omega NA\mu_o}{\sqrt{2}} \times 10^{-8} \frac{I_s}{I_m} \sqrt{1 - \left(\frac{I_s}{I_m}\right)^2} \frac{\text{RMS volts}}{\text{oersted}}$$

μ_o = linear permeability of core below saturation
in gauss/oersted

I_s = saturation current in amperes

A = cross sectional area of the core in square cm.

Paul J. Coleman, Jr. of Space Technology Laboratories, Inc., (presently with NASA) also presented a similar analysis (An Analysis of the Operation of the Fluxgate Magnetometer, 7320.2-14, 20 June 1959) except the hysteresis of the probe was taken into consideration. His result yielded,

$$e_o \approx k_2 H \frac{I_s}{I_m} \sqrt{1 - \left(\frac{I_s}{I_m}\right)^2 + k_1 \left(\frac{\delta}{I_m}\right)^2} \sin(2\omega t - \phi)$$

where

k_1 = constant

k_2 = proportionality constant and includes the probe constants

δ = the half width of the hysteresis loop of the core

measured along the H axis

$$\phi = \arctan \frac{K_3 I_s I_m \delta}{2 I_s I_m^2 - I_s^3}$$

K_3 = constant

δ introduces a small but constant phase shift as well as effecting the probe sensitivity slightly. It does not, however, alter the basic measurement. Note also that as δ approaches zero both solutions agree. In any case, the solutions show that e_o is proportional to H

thus achieving linear measurement of small field.

Other useful relations can be derived to facilitate probe design. If A or μ_o is difficult to determine but L_o (the inductance below saturation) can be selected or be made available,

$$L_o = 0.4\pi N^2 A \mu_e \times 10^{-8} / \ell$$

where

μ_e = effective permeability

$$\begin{aligned} & \propto \mu_o \text{ due to demagnetization effect} \\ & \propto \ell^2 / A \\ & = k_4 \ell^2 / A \end{aligned}$$

where

k_4 = constant of proportionality

Then,

$$k_4 = \frac{L_o 10^8}{0.4\pi N^2 \ell}$$

I_s is a function of winding geometry while B_m is constant for a given

core material. Hence,

$$I_s = \frac{B_m NA}{L_o} \times 10^{-8}$$

$$= \frac{B_m}{0.4 \pi N k_4 \ell}$$

From these parameters e_o can be determined.

To determine the sensitivity of the probe as a function of the driving current,

$$\frac{dS_2}{dI_m} = \frac{I_s}{I_m} \sqrt{1 - \left(\frac{I_s}{I_m}\right)^2}$$

Figure 26. shows the plot of this function. Maximum sensitivity is obtained when,

$$I_m = \sqrt{2} I_s$$

For this condition

$$\frac{d^2 S^2}{dI_m^2} = 0$$

The operating point is, therefore, usually selected at this point.

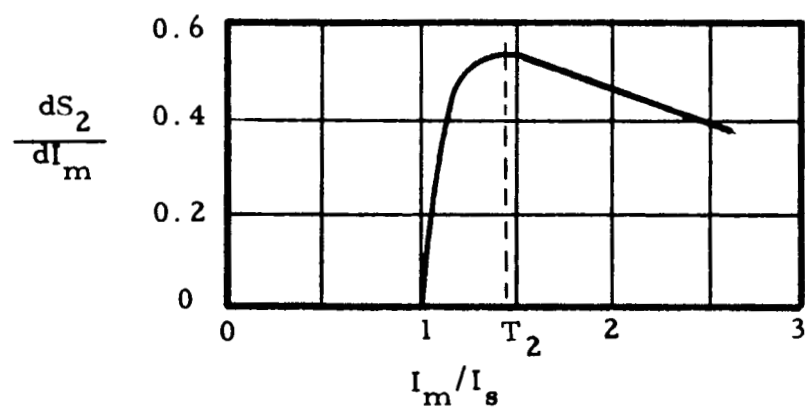


Figure 26. Probe Sensitivity Versus Drive Current Curve

APPENDIX B

TEST PROCEDURES:

S 40064

S 40079

1. USE		PARIS DISPOSITION		5.		S40064	
2. REWORK		3. CANNOT BE REWORKED		4. RECORD			
REVISIONS							
DISP	EFF	SYM	DESCRIPTION			BY	DATE

CMG LTR

S40064

[illegible]

1. SCOPE

1.1 This test procedure covers the Mariner R Magnetometer Checkout Unit (ML104-1) modified for Mariner R Magnetometer checkout. Its function is to monitor pertinent outputs, generate magnetic field, and simulate spacecraft command signals.

2. APPLICABLE DRAWINGS

S40003	Test Procedure, Test Set - Magnetometer ML104-1
T50067	Test Set Assembly - Triaxial Fluxgate Magnetometer
T50031	Schematic - Triaxial Fluxgate Magnetometer Flight Checkout Case
50144	Wiring List - Triaxial Fluxgate Magnetometer Flight Checkout Case
T50156	Cable Harness - Test Set Assembly
SP30003-101	Blank, Panel and Carrying Case Assembly
SP30004-101	Case Assembly - Panel Mounting
SP30005-101	Panel Assembly - Lower Blank
SP30006-101	Panel Assembly - Lid, Blank
50141	Terminal Board No. 1 Assembly - Triaxial Fluxgate Magnetometer Test Set
T50118	Terminal Board No. 1 Triaxial Fluxgate Magnetometer Test Set

RELEASE	DATE	TITLE	MARSHALL LABORATORIES
PREPARED		Test Procedure,	
G. Takahashi	12-15-61	Test Set -	
CHECKED		Magnetometer ML104-1	
APPROVED		Modified for Mariner R	
			NO.
			S40064
			SHEET 2 OF 10

CHG LTR

S40064

50142 Terminal Board No. 2 Assembly - Triaxial
Fluxgate Magnetometer Test Set

T50119 Terminal Board No. 2 Triaxial Fluxgate
Magnetometer Test Set

50143 Terminal Board No. 3 Assembly - Triaxial
Fluxgate Magnetometer Test Set

50120 Terminal Board No. 3 Triaxial Fluxgate
Magnetometer Test Set

50288 Schematic - Mariner R Checkout Adapter Unit,
Mariner R Checkout Adapter Unit Assembly

3. TEST EQUIPMENT

3.1 Standard. The following test equipment (or equivalent) is required.

3.1.1 Square wave power supply - Consolidated Systems Corporation
Type SC3192A.

3.1.2 Digital voltmeter - Non Linear Systems Model 481

3.1.3 Multimeter - Triplet Model 630NA

3.2 Non-Standard. The following test equipment is not available
commercially. It has been designed by Marshall Laboratories for specific tests.

3.2.1 Cylindrical Fluxtank ML102-1

3.2.2 Spherical Fluxtank ML103-1

3.2.3 Equivalent magnetic shield is desirable if available to reduce the
ambient magnetic field to "zero".

RELEASE	DATE	TITLE	MARSHALL LABORATORIES
PREPARED	12-15-61	Test Procedure,	
G. Takahashi		Test Set-	
CHECKED		Magnetometer ML104-1	
APPROVED		Modified for Mariner	
			NO. S40064 SHEET 3 OF 10

4. TESTS REQUIRED AND TEST SETUPS

4.1 Preliminary Suitcase Test

4.1.1 Measure voltage at 3 test points marked 1 volt. This voltage should be monitored and adjusted periodically by adjusting R4, R17, and R30. These potentiometers are subpanel mounted.

(a) Flip 3 calib. field supply toggle switches to "on". (located in upper right hand corner).

(b) Turn 3 calib. field switch to + position.

4.1.2 Test point marked +12 monitors the power supply regulator output and must be set to +12.00 v d-c by adjusting R54 which is subpanel mounted.

(a) Flip + 12 toggle switch to "on".

(b) Meter selector switch to be in position "1" (+ 12v).

(c) Meter should read 87% of full scale.

(d) Also + 12 can be monitored by external meter at + 12 jacks in upper right hand corner.

4.1.3 Test point marker -12 is a nominal value and should be between -12 to -15 volts.

(a) Turn -12 Toggle switch to "on".

(b) Measure -12 with external meter at -12 jacks in upper right hand corner. Reading should be between -12 to -15 volts.

4.1.4 Battery charger. The unit contains a taper charger designed to recharge the batteries in 10 to 12 hours. Recharging is required whenever the

RELEASE	DATE	TITLE	MARSHALL LABORATORIES
PREPARED G. Takahashi	12-15-61	Test Procedure,	
CHECKED		Test Set -	
APPROVED		Magnetometer ML104-1	
		Modified for Mariner R	
			NO.
			S40064
			SHEET 4 OF 10

+12 or -12 test points indicate low voltage.

4.1.4.1 Recharging Procedures

1. CHARGE OPERATE switch to CHARGE
2. Insert jumpers of milliameters into CHARGING CURRENT test points. +12 (10 to 400 ma); -12 (10 to 250 ma).

3. Remove battery caps
4. Connect a-c line cord to panel and 115 v a-c 50/60 cps.
5. Charge for 10 to 12 hours.

4.2 Test set-up for complete system checks. See Figure 1 for test set-up.

4.2.1 Suitcase Control Settings.

NULL FIELD - OFF

CALIB. FIELD - OFF

VARIABLE - OFF

A-C FIELD AMP - OFF

+12 Toggle switch - ON

-12 toggle switch - ON

POWER toggle switch - INT

CALIB FIELD SUPPLY toggle switches - ON

CHARGE OPERATE switch - OPERATE

COMMAND switch (S2) on adapter unit in command 3 position.

Meter selector - Position 3 (Spectrum 3). Meter monitors

RELEASE	DATE	TITLE	MARSHALL LABORATORIES
PREPARED G. Takahashi	12-15-61	Test Procedure, Test Set -	
CHECKED		Magnetometer ML104-1	
APPROVED		Modified for Mariner R	
			NO. S40064
			SHEET 5 OF 10

calibrate indicator output.

Pulse selector - Position 1 (In flight calibration)

Depress and release pulse push button switch S23. Meter should read zero.

4.3 "Zero" field Set-up (applicable for each axis). Remove all magnetic materials from probe vicinity. If fluxtanks are not used, zero condition may not be attained due to excessive ambient field fluctuation.

4.3.1 NULL FIELD to +.

4.3.2 Adjust COARSE and FINE control slowly to bring DATA meter toward center scale. If DATA meter deflects away from center scale, reverse the polarity (NULL FIELD to -).

4.3.3 Zero field condition is indicated by DATA meter at center scale and SCALE meter on scale 1 (approximately 45% of full scale).

5. PERFORMANCE REQUIREMENT

5.1 Power Supply.

5.1.1 Apply primary power and measure supply output for + 12.00 v d-c \pm 0.2% as marked on adapter unit.

5.1.2 Fine adjustment can be made on the magnetometer unit as labeled.

5.2 Magnetic Field Measurement (applicable for each axis).

5.2.1 Procedure

1. Adjust for zero field (Section 4.3)

RELEASE	DATE	TITLE	MARSHALL LABORATORIES
PREPARED G. Takahashi	12-15-61	Test Procedure, Test Set -	
CHECKED		Magnetometer ML104-1	
APPROVED		Modified for Mariner R	
			NO. S40064
			SHEET 6 OF 10

CHG LTR

S40064

2. Depress Lo pushbutton switch located on adapter unit

DATA meter - 35 or 65% of full scale

SCALE meter - 45% of full scale

Release LO switch

3. Depress HI pushbutton switch located on adapter unit.

DATA meter - 35 or 65% of full scale

SCALE meter - zero

Release Hi switch

4. Note: Data output will be a function of probe cable length; longer the cable lower the output. Total cable capacity should be 185 ± 10 mmf.

CALIB FIELD to +.

5. The VARIABLE control on the Test Set may be used to generate adjustable magnetic field. (Turn CALIB FIELD to + or -)

6. Depress and hold SENSOR SHORT push button switch (S1) located on adapter unit.

DATA meter - 50% of full scale

SCALE meter - 45% of full scale

Release switch

5.3 In-flight Calibration Checkout.

5.3.1 Procedure

1. Adjust for zero field (Section 4.4)
2. COMMAND SWITCH (S2) on adapter unit to command 1 position.

RELEASE	DATE	TITLE	MARSHALL LABORATORIES
PREPARED	G. Takahashi 12-15-61	Test Procedure,	
CHECKED		Test Set-	
APPROVED		Magnetometer ML104-1	
		Modified for Mariner R	
NO. S40064			SHEET 7 OF 10

CHK LTR

S40065

3. METER SELECTOR to position 3 (Spectrum 2).
4. PULSE SELECTOR to position 1.
5. Depress and release PULSE push button switch.

DATA meter - 35 or 65%

SCALE meter - 45% of full scale.

METER - 100% of full scale.

6. COMMAND switch (S2) on adapter unit to command 3 position.
7. Depress and release PULSE push button switch.

DATA meter - 50% of full scale.

SCALE meter - 45% of full scale.

METER - 10% of full scale.

5.4 Temperature Monitor. The temperature data output indicates the nominal electronics temperature. A nominal temperature vs. output relation is shown below.

5.4.1 Procedure

1. METER SELECTOR to position 2 (Spectrum 1). METER now monitors temperature data output with 6 volts full scale.

2. Nominal temperature vs. meter relation is as follows:

<u>°F</u>	<u>OUTPUT - vdc</u>
0	6
25	5.3
50	4.2
75	3
100	2.2
125	1.4
150	1.0

6. QUALITY ASSURANCE PROVISIONS

RELEASE	DATE	TITLE	MARSHALL LABORATORIES	
PREPARED	G. Takahashi	12-15-6		NO. S40065
CHECKED				
APPROVED				
			SHEET 8 OF 10	

Test Procedure
Test Set -
Magnetometer ML104-1
Modified for Mariner R

6.1 The tests described in section 5 shall be applied to every magnetometer unit.

7. NOTES

CHG LTR

S40064

RELEASE	DATE	TITLE	MARSHALL LABORATORIES
PREPARED		Test Procedure,	
G. Takahashi	12-15-61	Test Set -	
CHECKED		Magnetometer ML104-1	
APPROVED		Modified for Mariner R	
			NO. S40064
			SHEET 9 OF 10

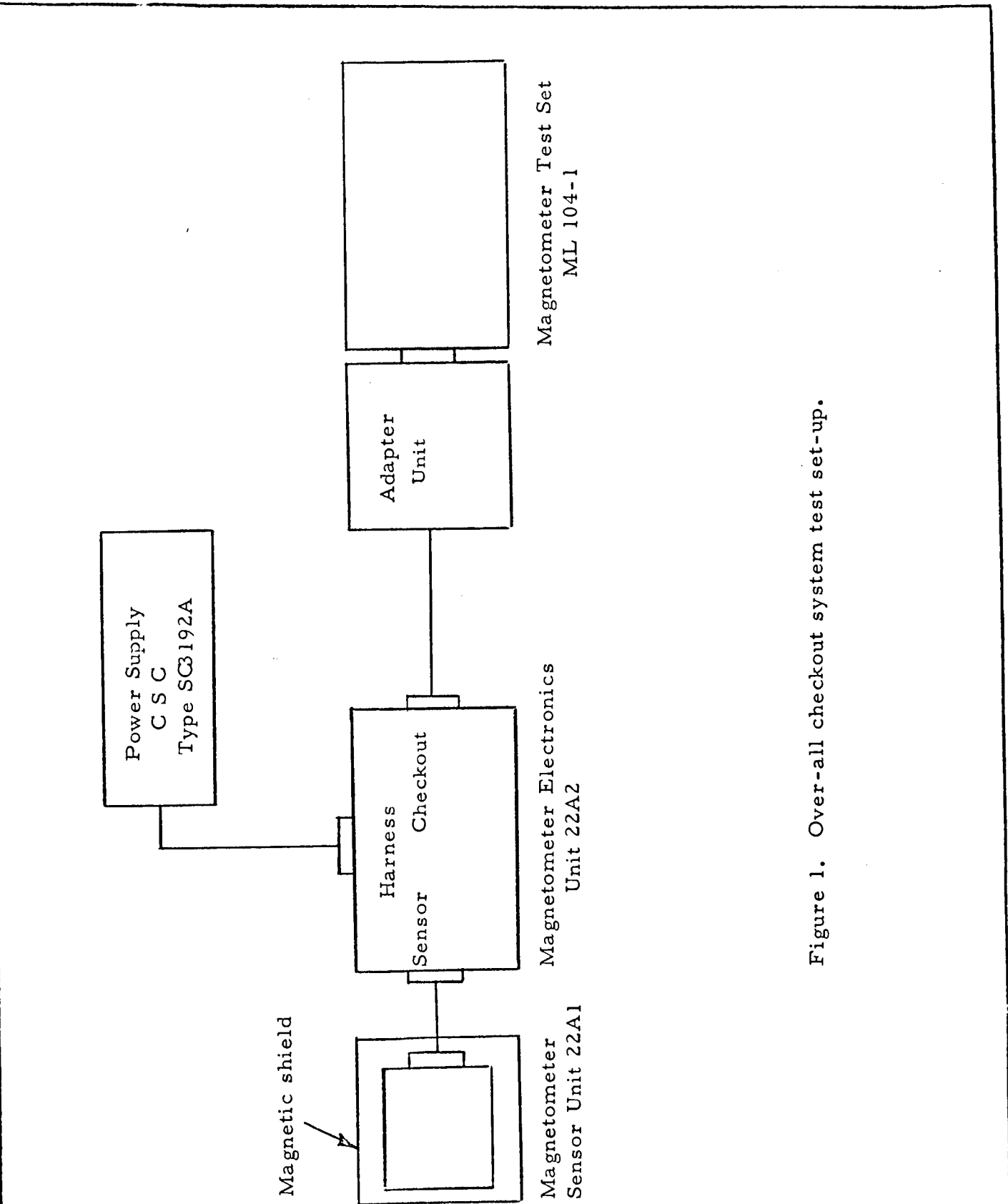


Figure 1. Over-all checkout system test set-up.

RELEASE	DATE	TITLE Test Procedure, Test Set - Magnetometer ML104-1 Modified for Mariner R	MARSHALL LABORATORIES	
PREPARED				
G. Takahashi	12-15-61		NO.	S40064
CHECKED			SHEET	10
APPROVED			OF	10

CHG LTR

S 40079

RELEASE	RELEASED	DATE 14	TITLE	MARSHALL LABORATORIES
PREPARED	R. Kobayashi	12/7/61	Tune-Up and Final Calibration Procedure.	
CHECKED	<i>R. Kobayashi</i>	<i>12/12/61</i>	Mariner R Fluxgate Magnetometer	
APPROVED	<i>R. Kobayashi</i>	<i>12/12/61</i>		
				NO.
				S 40079
				SHEET i OF 11

CHS LTR

S 40079

1. SCOPE

1.1 This procedure covers the initial tune-up and final calibration of the Mariner R Fluxgate Magnetometer, ML 126-1.

2. APPLICABLE DOCUMENTS AND DRAWINGS

2.1 50227, Schematic Diagram, (sheet 1 and 2).

2.2 S40064, Test Procedure, Mariner R Fluxgate Checkout unit.

2.3 40065, Test Procedure, Magnetometer Control, ML 141-1.

2.4 50243 Module assembly, fluxgate.

2.5 50246 Module assembly, power supply and in-flight calibrate.

3. TEST EQUIPMENT

3.1 Standard. The following test equipment or their equivalent is required.

3.1.1 Oscilloscope, Tektronix, Type 535

3.1.2 Oscilloscope preamp, Tektronix, Type CA

3.1.3 Digital Voltmeter, Non-Linear System, Model 481

3.1.4 Temperature Chamber, Tenny Engineering, Model TMUF-100240

3.1.5 Signal Generator, Hewlett-Packard, HP 202A

3.1.6 Counter, Hewlett-Packard, HP 512A

3.1.7 Multimeter, Triplet, 630NA

3.1.8 Power Supply, Consolidated System Corporation, Type CSC3192A.

3.1.9 Power Supply, Hewlett-Packard, HP 721

3.1.1.0 Decade Resistor, General Radio, Type 1432-L

3.1.1.1 Decade Capacitor, General Radio, Type 1419-A

3.2 Non-Standard. The following test equipment is not available commercially. It has been designed by Marshall Laboratories for specific tests.

RELEASE	RELEASED	DATE	TITLE	MARSHALL LABORATORIES NO. S 40079 SHEET 1 OF 11
PREPARED	R. Kobayashi	12/7/61	Tune-Up and Final Calibration Procedure.	
CHECKED			Mariner R Fluxgate Magnetometer.	
APPROVED				

CXG LTR

S 40079

- 3.2.1 Spherical fluxtank
- 3.2.2 Triaxial Helmholtz coil array
- 3.2.3 Triaxial Helmholtz coil array electronics
- 3.2.4 Dummy load and milliammeter
- 3.2.5 Mariner R checkout unit
- 3.2.6 Data and scale meters.

4. PRELIMINARY SETUP PROCEDURE

4.1 Initial Fluxgate Tune-Up.

4.1.1 See Figure 1.

4.1.2 This test is performed to select C and R values for optimum circuit operation.

4.1.3 Use signal generator to find band pass filter center frequency.

- (1) board #1, 32KC
- (2) board #2, 40KC
- (3) board #3, 48KC

4.1.4 Tune transformers and inductors.

- (1) T3; select oscillator C25, 26 to bandpass filter center frequency.
- (2) T6; select signal push-pull amplifier C46, 47 for maximum signal.
- (3) L1; select phase shift network C32, 33 such that the output signal equals the input signal.
- (4) L2; select phase control C36, 37 such that the output equals input signal. When R37 is varied from minimum to maximum resistance, the output signal should not change amplitude but shift in phase 180 degrees.
- (5) T4; select reference amplifier C39, 40 for maximum signal.
- (6) T2; select scale switch amplifier C14, 15 for maximum signal.

RELEASE	RELEASED	DATE	TITLE	MARSHALL LABORATORIES
PREPARED	R. Kobayashi	12/7/61	Tune-Up and Final Calibration Procedure.	
CHECKED			Mariner R Fluxgate Magnetometer.	
APPROVED				
				NO.
				S 40079
				SHEET 2 OF 11

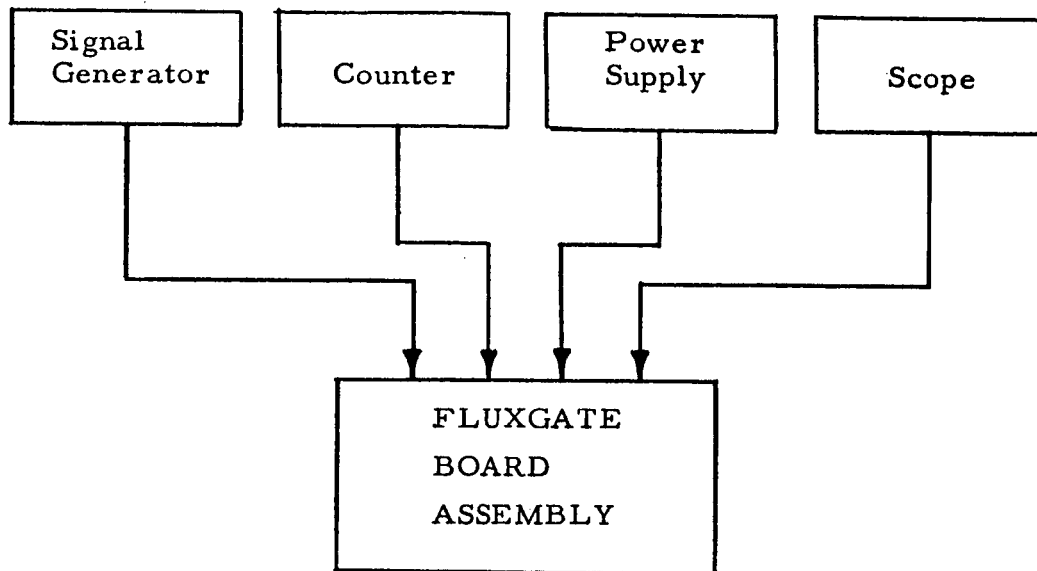


Figure 1. Set Up For Initial Fluxgate Tune Up.

4.1.5 Let R32 be 1.5K; select R32 such that Z13 (reference amplifier) just starts to saturate.

4.1.6 Let R40 be 110K.

4.2 Fluxgate Probe Drive Setup.

4.2.1 See Figure 2.

4.2.2 Each board to be tuned to their respective probe axis and frequency.

4.2.3 Set R1, 2 to 10K; R3, 4 to 100K; and R5, 6 to 510 ohms.

4.2.4 Vary balance pot R9 for minimum input B+ current. (approx. 60 to 65 ma).

4.2.5 Vary C3, 4, 5 for maximum signal across T1 primary. Switching transients should be near zero crossover.

4.2.6 Vary probe secondary tuning C6, 7, 8 for maximum signal at Q4.

4.2.7 Adjust phase control, R37, for maximum d-c data output.

4.2.8 Short probe secondary, adjust R44 for 3.5 V d-c output bias level.

4.2.9 Change polarity of applied field for output symmetry. Re-adjust C3, 4, 5 and C6, 7, 8 as necessary. Output symmetry to be less than 100 mv for plus and minus fields.

4.2.10 Adjust R53 for ± 2 volt deflection about 3.5 V d-c for a ± 64 gamma field.

4.3 Scale Switching Setup.

4.3.1 With R16 in mid-position, select R14 such that the scale switching circuit will activate at about 72 gamma.

4.3.2 Adjust R47 for full scale deflection of $\pm 2V$ d-c about 3.5V d-c for a ± 320 gamma field.

4.4 I. F. C. and Power Supply Setup and Final Calibration.

4.4.1 See Figure 3.

4.4.2 This test is performed to set up and check operation of the in-flight calibrate system, derive unit temperature curve, and for the final calibration of the ± 12 volt and -9 volt power supply.

RELEASE	DATE	FILE	Tune-Up and Final Calibration Procedure. Mariner R Fluxgate Magnetometer.	MARSHALL LABORATORIES
PREPARED				
R. Kobayashi	12/7/61			
CHECKED				
APPROVED				
				S 40079
			SHEET	4 OF 11

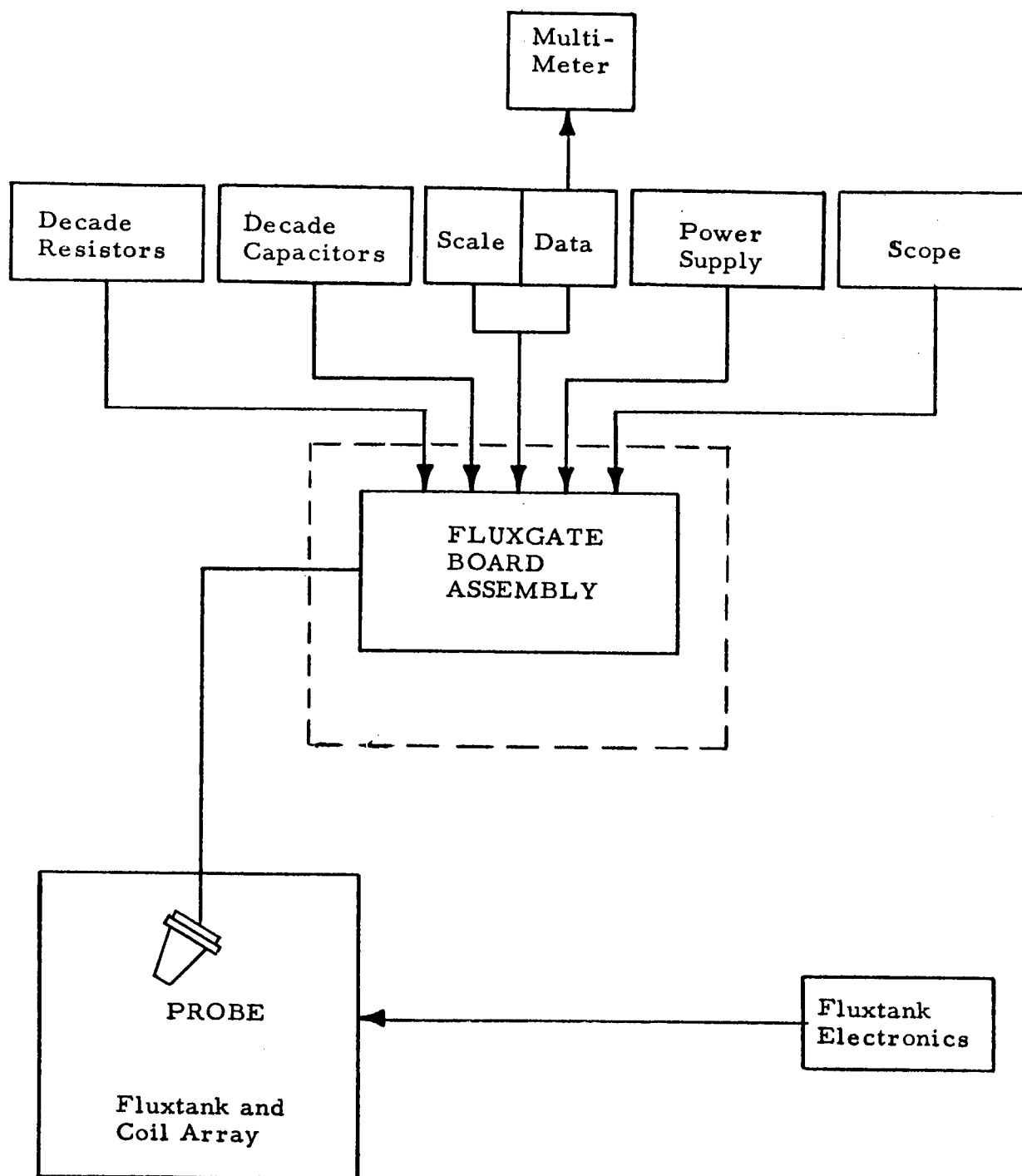


Figure 2. Tune-Up Of Fluxgate To Probe Setup.

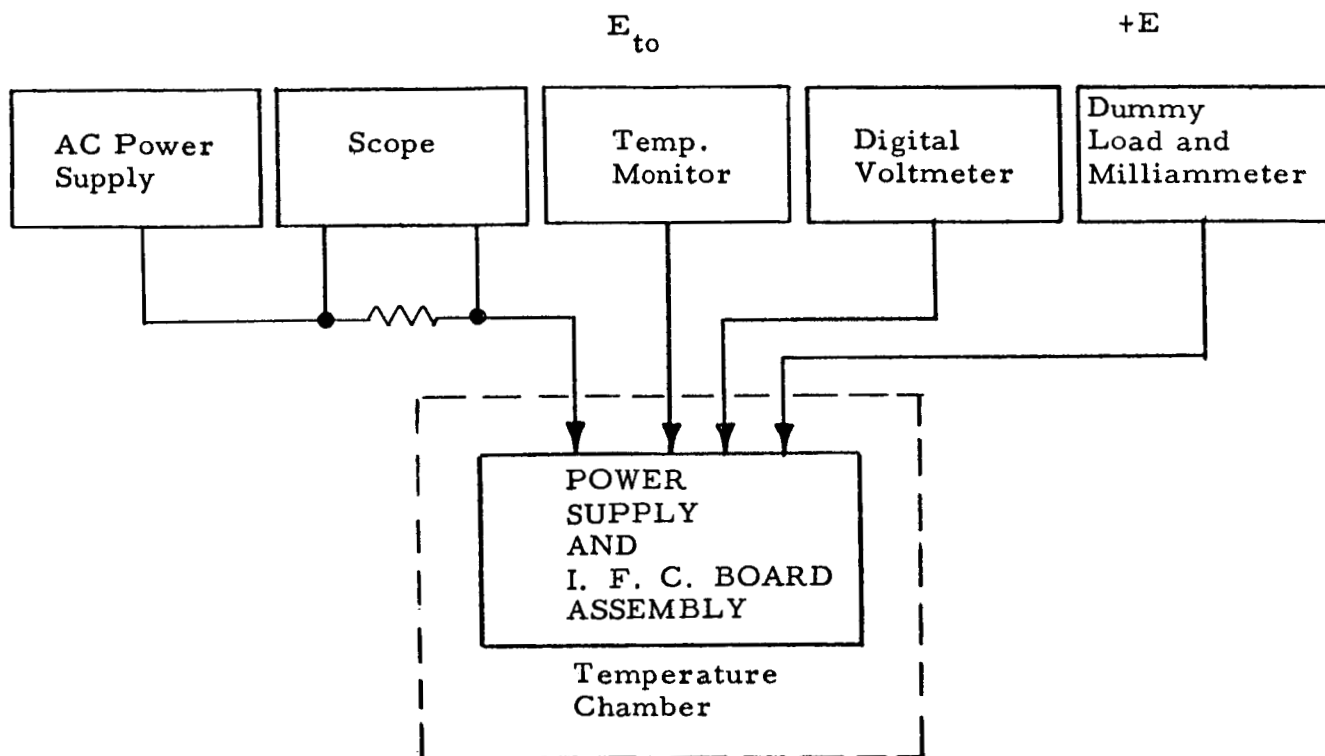


Figure 3. Power Supply And In-Flight Calibrate Setup.

4.4.3 Monitor AC input current to power supply across one ohm resistor.

4.4.4 Adjust R228 for 12.00v d-c $\pm 0.1\%$ output with load at 175 ma. Vary load from 50 to 300 ma d-c, output should not vary more than 20 mv. Select fuse, F200, 2 times nominal input current.

4.4.5 Monitor -9.0v d-c $\pm 5\%$ supply with steady 3 ma load output should not vary more than $\pm 0.1\%$ over test temperature range.

4.4.6 Let R 203, 216, 217, be 750K. I. F. C. point is 32 gamma.

4.4.7 Trigger I. F. C. with a 5-volt negative pulse. Output should deflect approximately 1 volt.

4.4.8 Reset I. F. C. with a 5 volt negative pulse.

4.4.9 Monitor above tests from 0° to 150°F in 30°F increments of temperature while deriving the unit temperature sensor characteristics.

4.5 Probe Drive Temperature Compensation.

4.5.1 See Figure 4.

4.5.2 This test is to select the final resistor values (R1, 2, 3, 4, 5 and 6) for the probe drive temperature compensation.

4.5.3 Adjust R_p (R1, 2) at 0°F temperature for full scale output.

4.5.4 Adjust R_s (R3, 4) at 150°F temperature for full scale output.

4.5.5 Vary R_d (R5, 6) to verify R_p and R_s for full scale output.

4.5.6 Repeat temperature cycling between 0, 75 and 150°F as necessary until the best compensation can be derived. At extreme temperatures, full scale variations should be less than 250 mv.

4.5.7 Recheck and/or alter all variable potentiometers to obtain optimum results.

5.0 FINAL CALIBRATION PROCEDURE

5.1 See Figure 5.

5.2 Readjust gain, bias and phase controls to proper points as necessary.

5.3 The following tests are made at 0, 75, and 150°F .

5.4 Magnetic Field versus Data Input Calibration (H_o vs E_o)

RELEASE	RELEASED	DATE 14 1961	TITLE	MARSHALL LABORATORIES
PREPARED	R. Kobayashi	12/7/61	Tune-Up and Final Calibration Procedure.	
CHECKED			Mariner R Fluxgate Magnetometer.	
APPROVED				
				NO. S 40079
				SHEET 7 OF 11

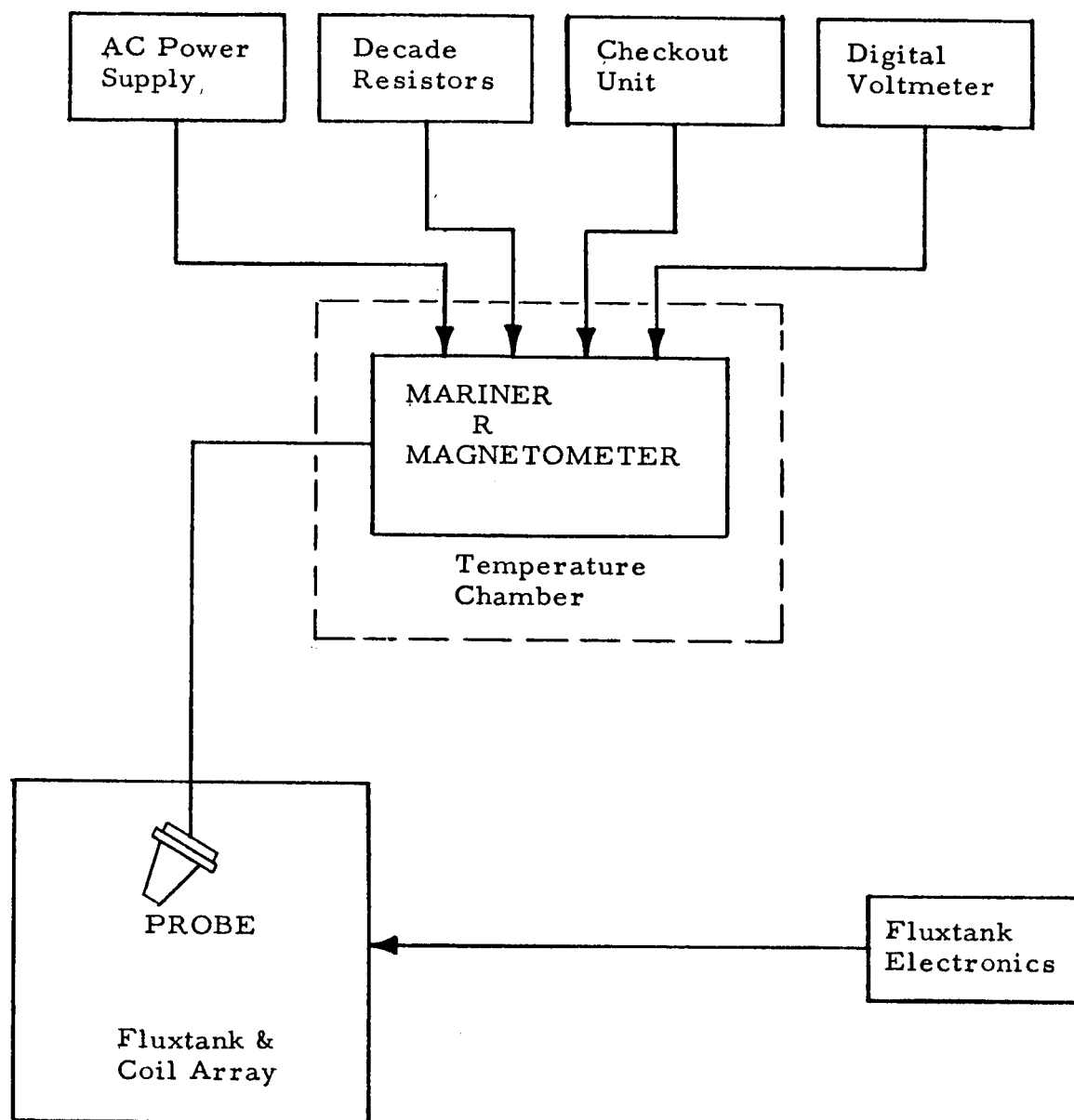


Figure 4. Fluxgate Magnetometer Temperature Compensation Setup.

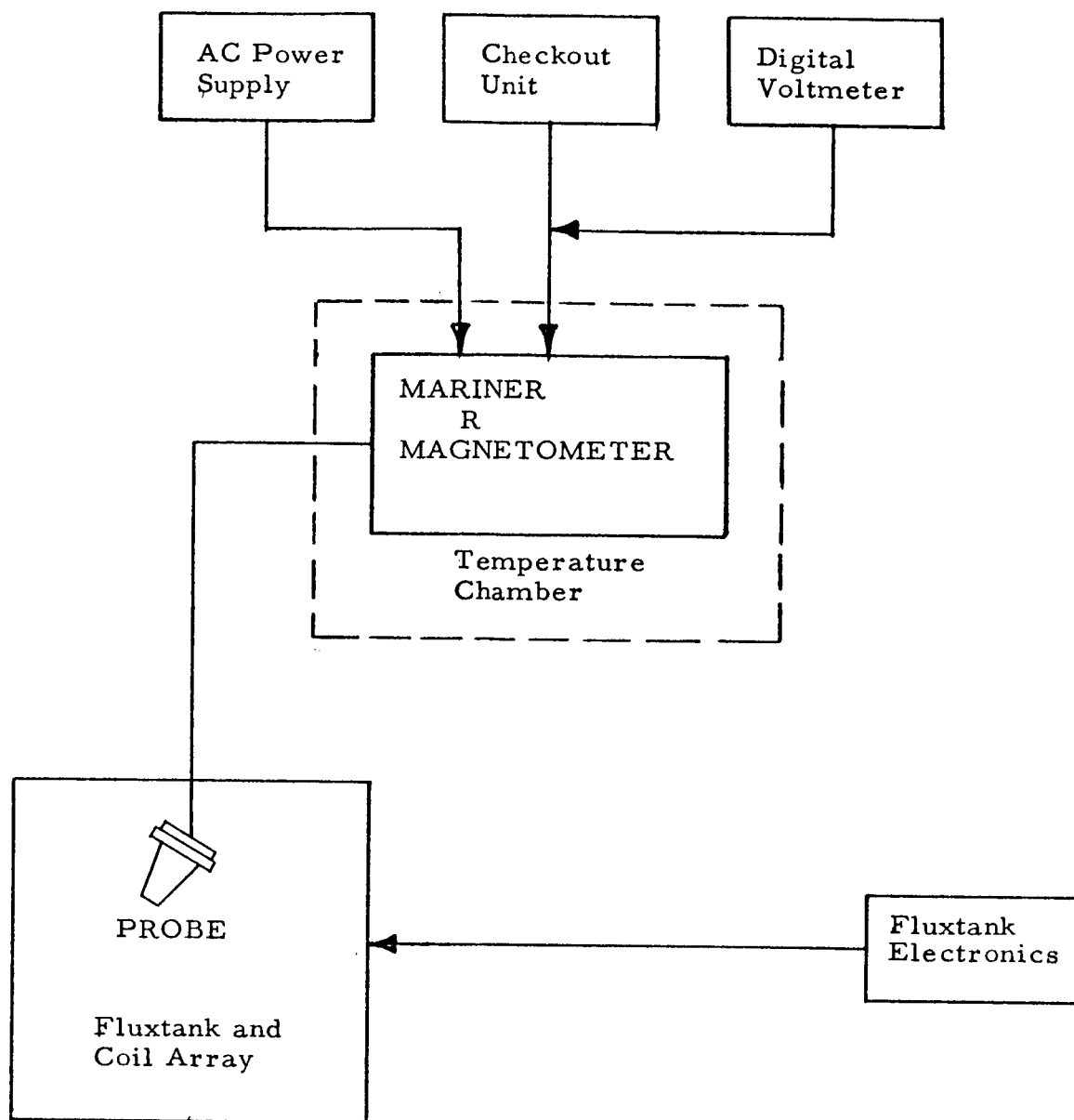


Figure 5. Final Calibration Mariner R Magnetometer Setup.

CHS LTR

S 40079

5.4.1 Scale 1, ± 2 volts about 3.5v d-c for ± 64 gamma.

5.4.2 Scale 2, ± 2 volts about 3.5v d-c for ± 320 gamma.

5.4.3 Data points to be taken in 8 gamma increments for scale 1 and 40 gamma increment for scale 2.

5.4.4 Scale indication is noted by full scale deflection (11v d-c ± 0.5) for Scale 1 and zero deflection (0.3v d-c) for Scale 2.

5.4.5 Scale switching from scale 1 to scale 2 will occur near 1 or 6v d-c depending on the field polarity.

5.4.6 Activate I. F. C. circuit for each axis at the calibrating temperature. Record deflection and insert information on calibration curve (H_o vs E_o). Calibration point is approximately 32 gamma.

5.5 Perm Test Calibration

5.5.1 This test is performed to determine the perm offset of the probe and electronics.

5.5.2 The following procedure is applicable to each of the three axes.

5.5.2.1 Perm-50K gamma, null, record H1.

5.5.2.2 Flip probe, null, record H2

5.5.2.3 Perm -50K gamma, null, record H3.

5.5.2.4 Flip probe, null, record H4.

5.5.2.5 Perm-50K gamma, null, record H5.

5.5.3 From the above data the effect of a high field on probe and electronics can be determined.

5.5.3.1 Probe perm, $H_{p1} = \frac{H_3 - H_2}{2}$, $H_{p2} = \frac{H_5 - H_4}{2}$

5.5.3.2 Total perm, $H_{t1} = \frac{H_1 - H_2}{2}$, $H_{t2} = \frac{H_3 - H_4}{2}$

5.5.3.3 Electronic perm, $H_{e1} = H_{t1} - H_{p1}$, $H_{e2} = H_{t2} - H_{p2}$

RELEASE	DATE	TITLE	MARSHALL LABORATORIES
PREPARED	12/7/61	Tune-Up and Final Calibration Procedure. Mariner R Fluxgate Magnetometer.	
R. Kobayashi			
CHECKED			
APPROVED			
NO. S 40079			
SHEET 10 OF 11			

5.6 Temperature Calibration

5.6.1 This test was performed in section 4.4 Re-verify 0, 75, and 150°F points.

5.7 Power supply calibration

5.7.1 This test was performed in Section 4.4 Re-verify output voltages at 0, 75 and 150°F.

5.8 This concludes final calibration.

5.9 The following curves and test results are to be included in the unit history record.

5.9.1 Magnetic field versus data output, six curves with I. F. C. data points noted.

5.9.2 Power supply and temperature sensor characteristics, one power supply data table and one temperature versus output curve (T vs E_{to})

5.9.3 Apparent probe perm versus temperature, H_p versus T.

5.9.4 Orientation of probe with respect to the direction of the applied field (polarity)

6. QUALITY ASSURANCE PROVISIONS

6.1 The test herein described are applied to all magnetometer units developed under this program.

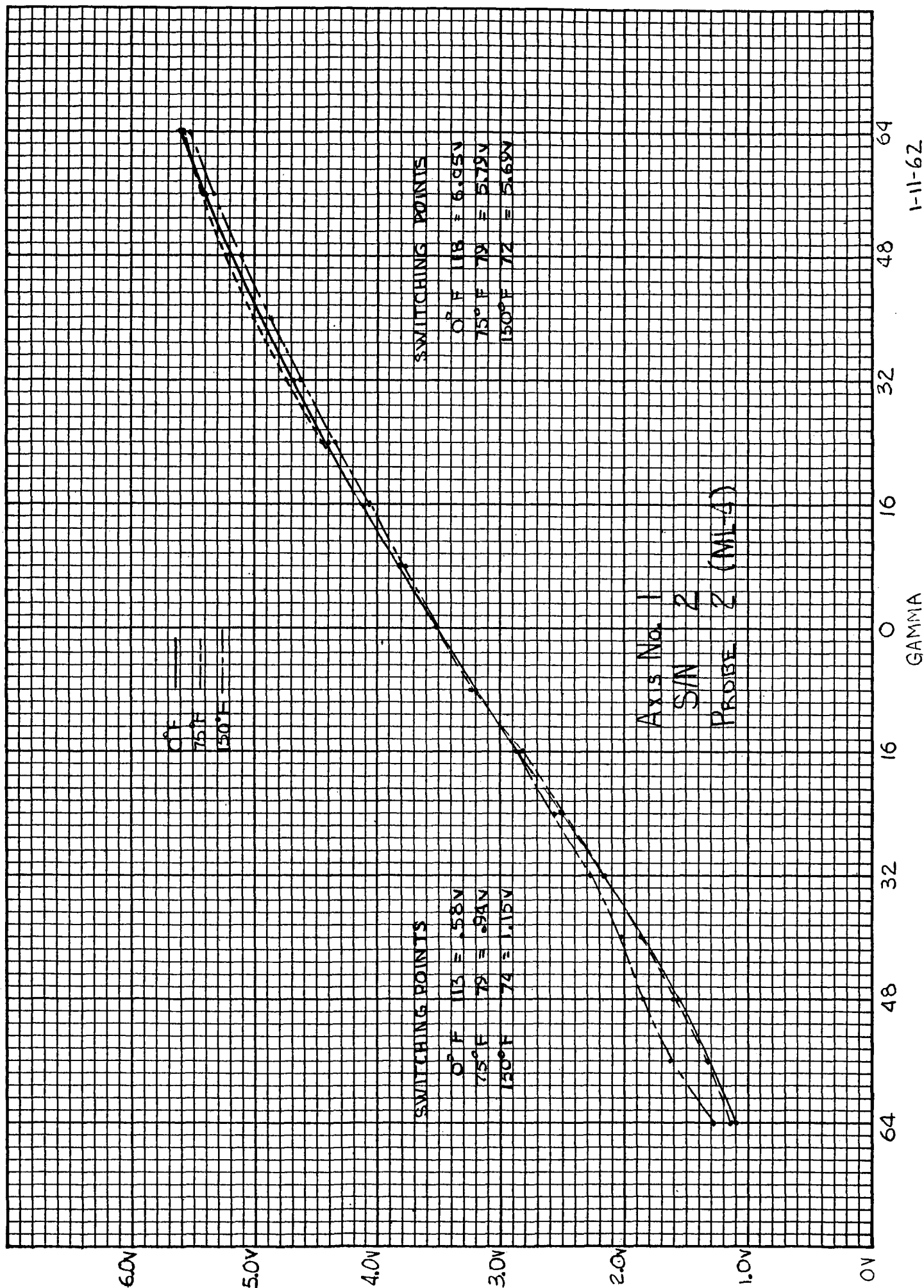
7. NOTES

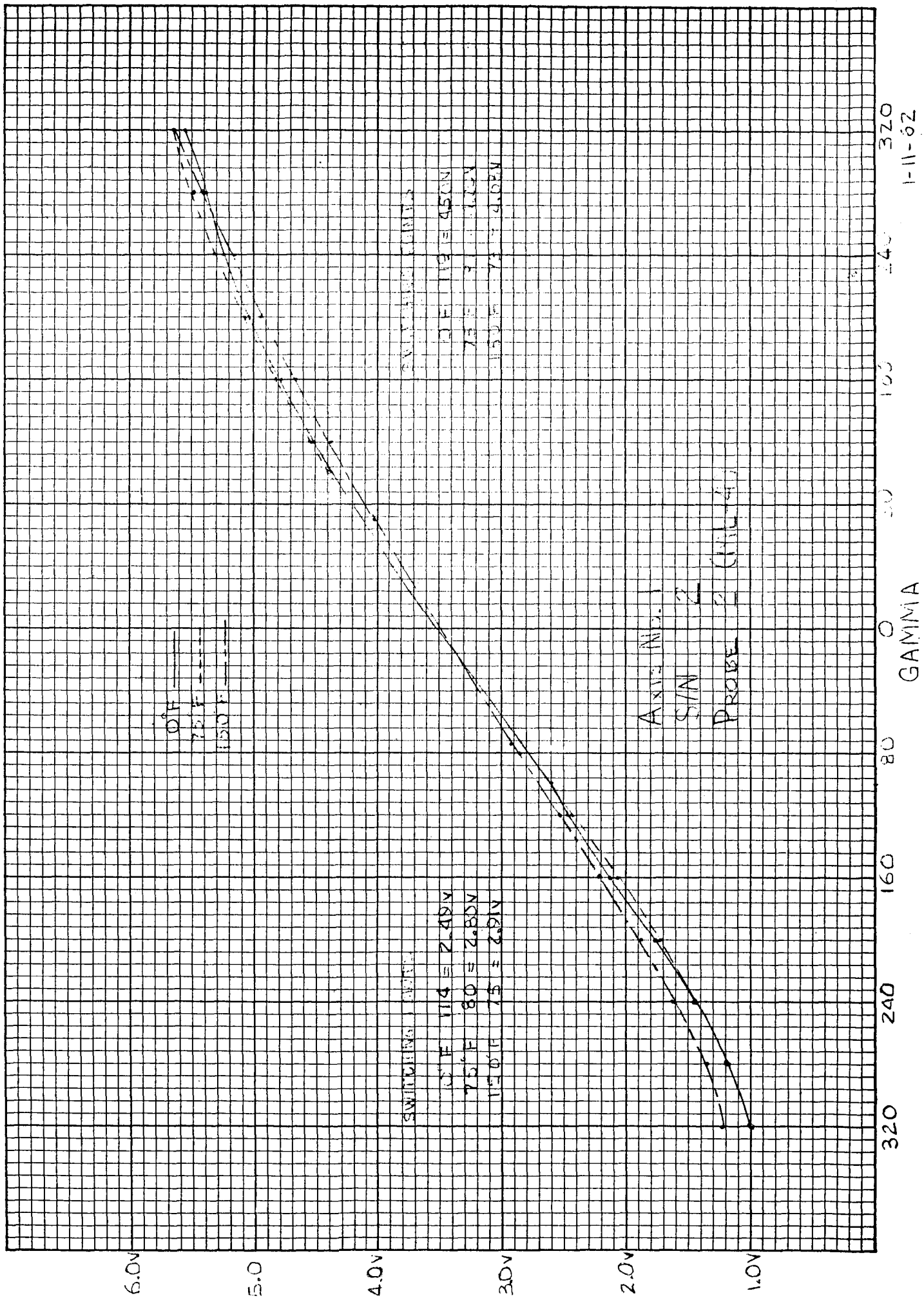
RELEASE	DATE 11 12 1961	TYPE	Tune-Up and Final Calibration Procedure. Mariner R Fluxgate Magnetometer	MARSHALL LABORATORIES
PREPARED R. Kobayashi	12/7/61			
CHECKED				
APPROVED				
				NO. S 40079
			SHEET 11	OF 11

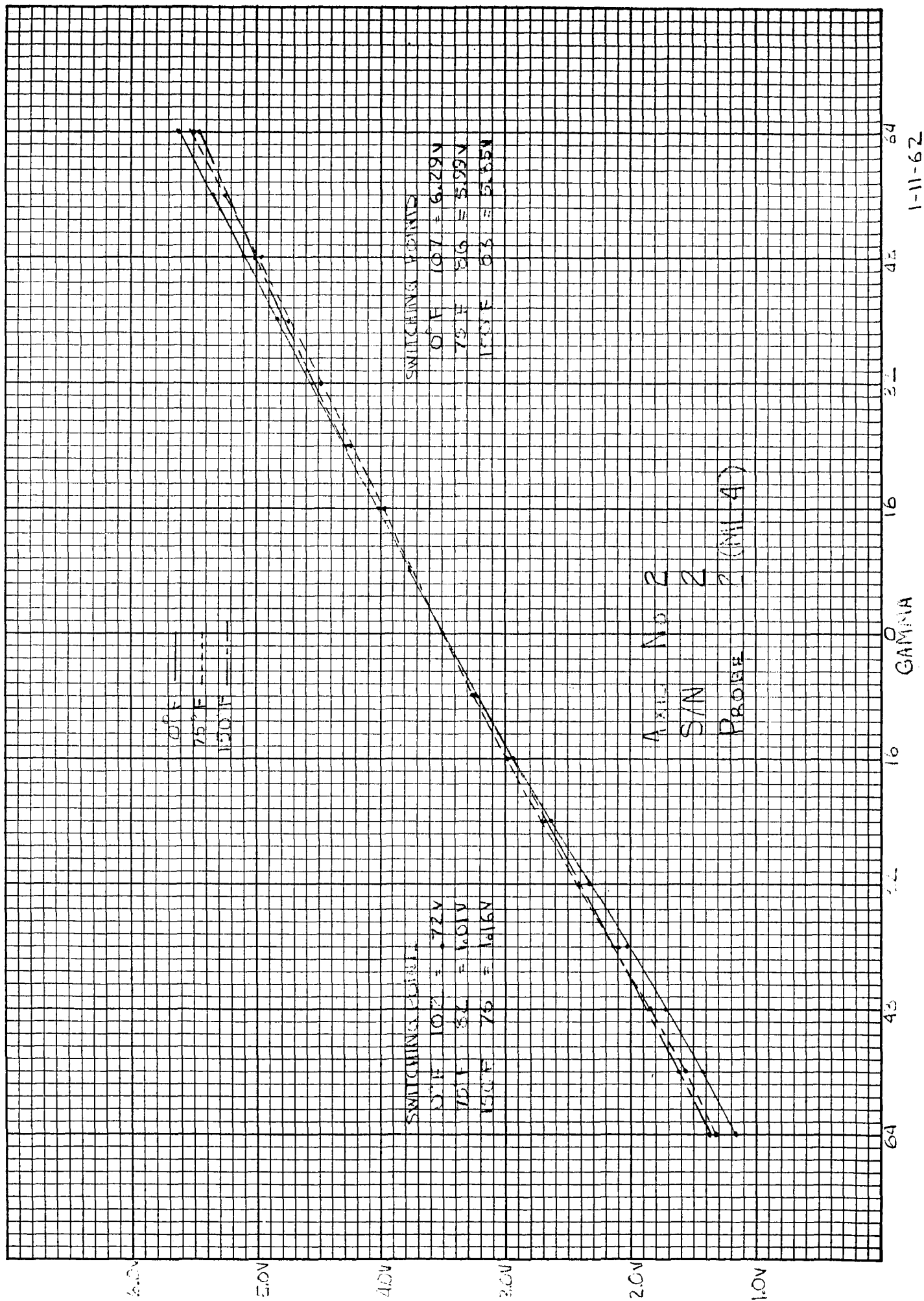
ML/TN - 2000.47
Page 86.

APPENDIX C
FINAL TEST RESULTS

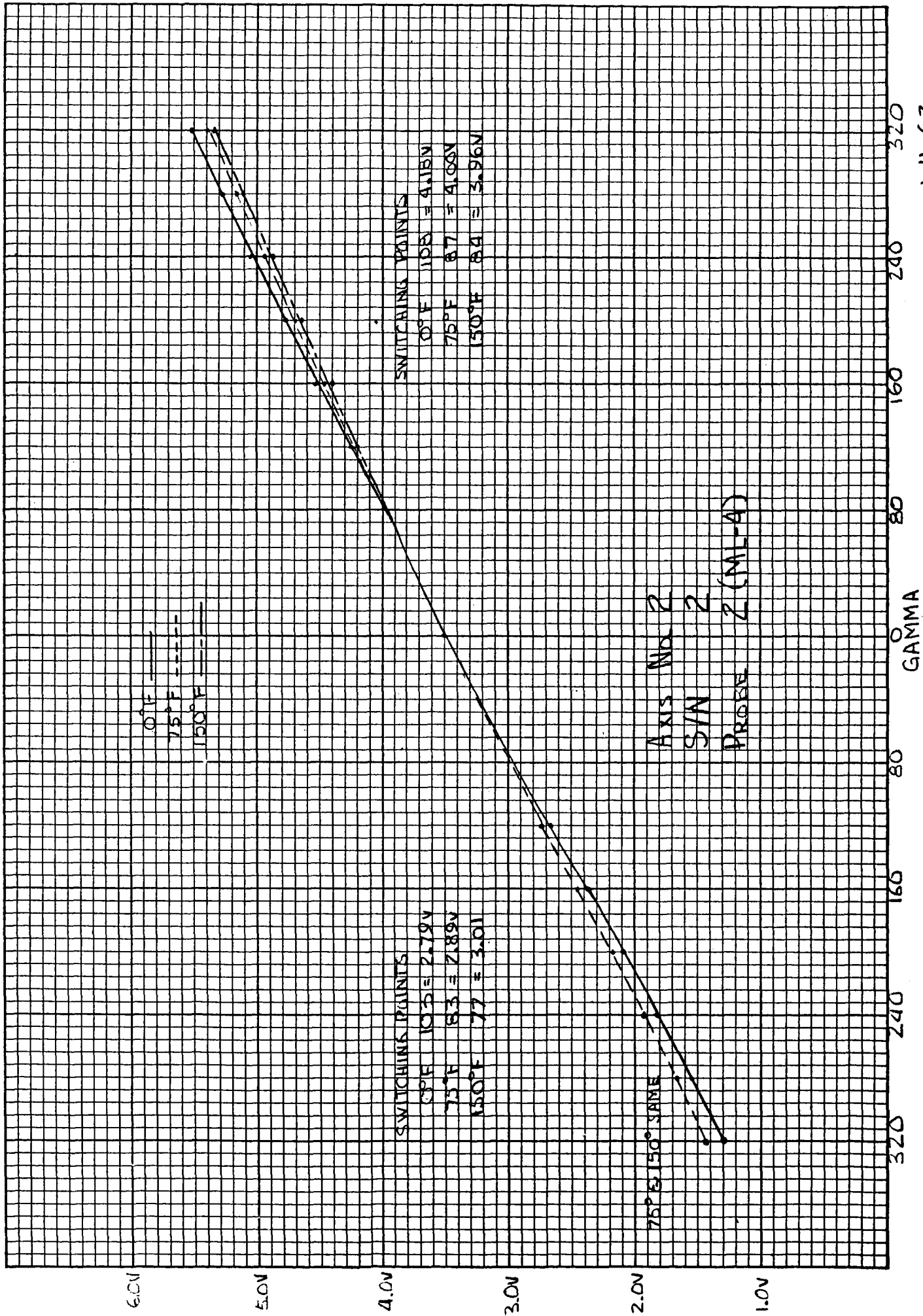
Master Drawing List

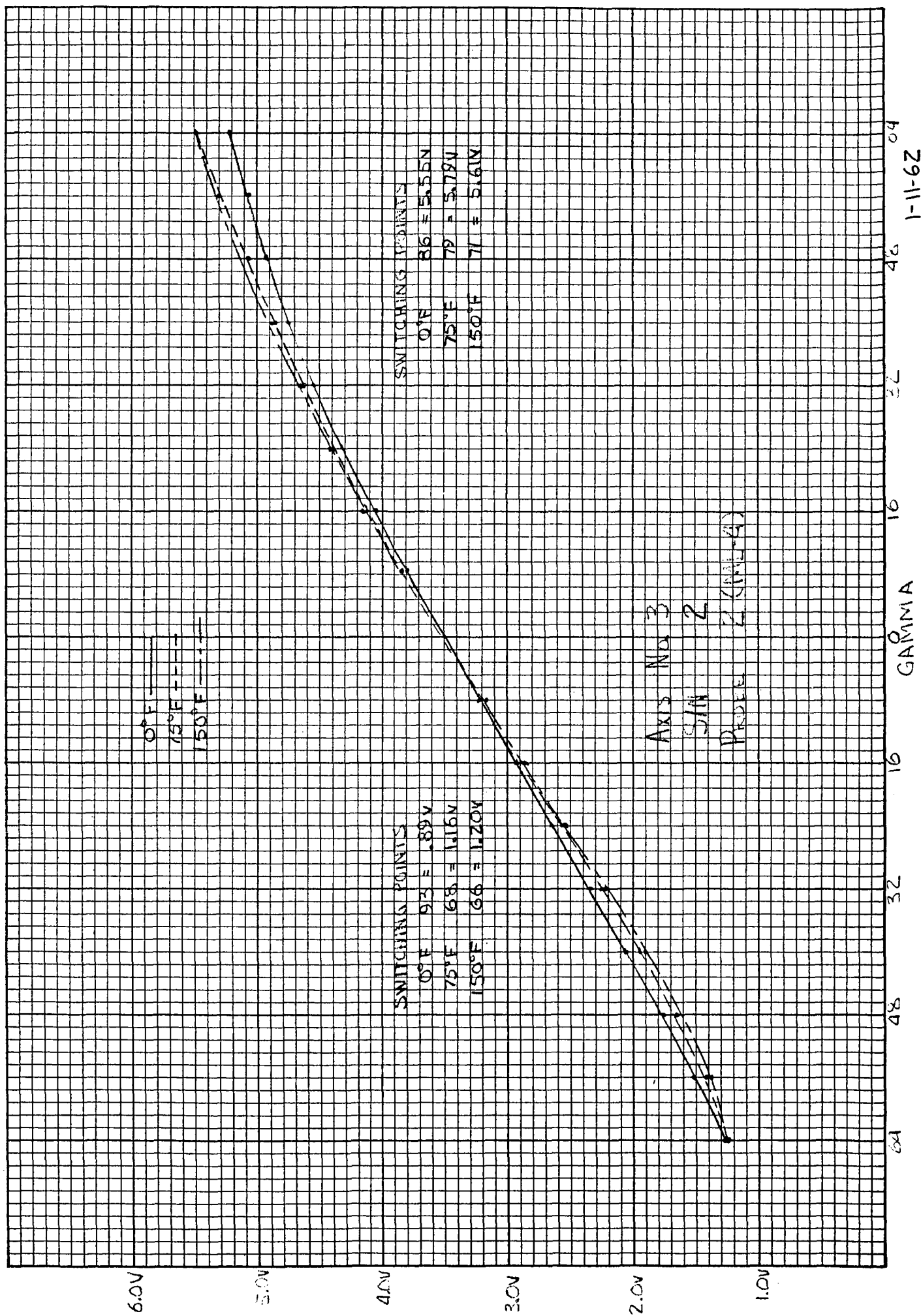


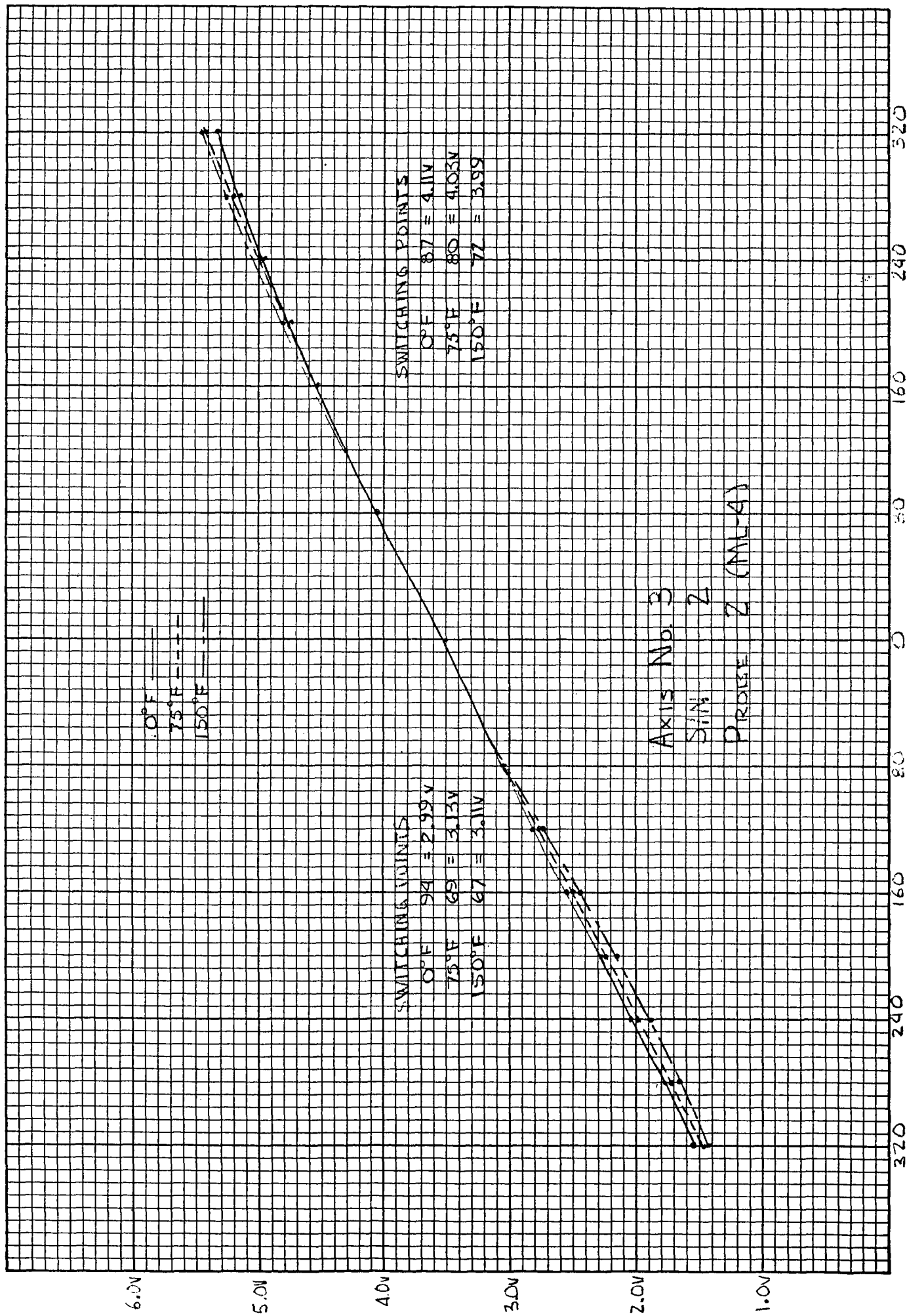


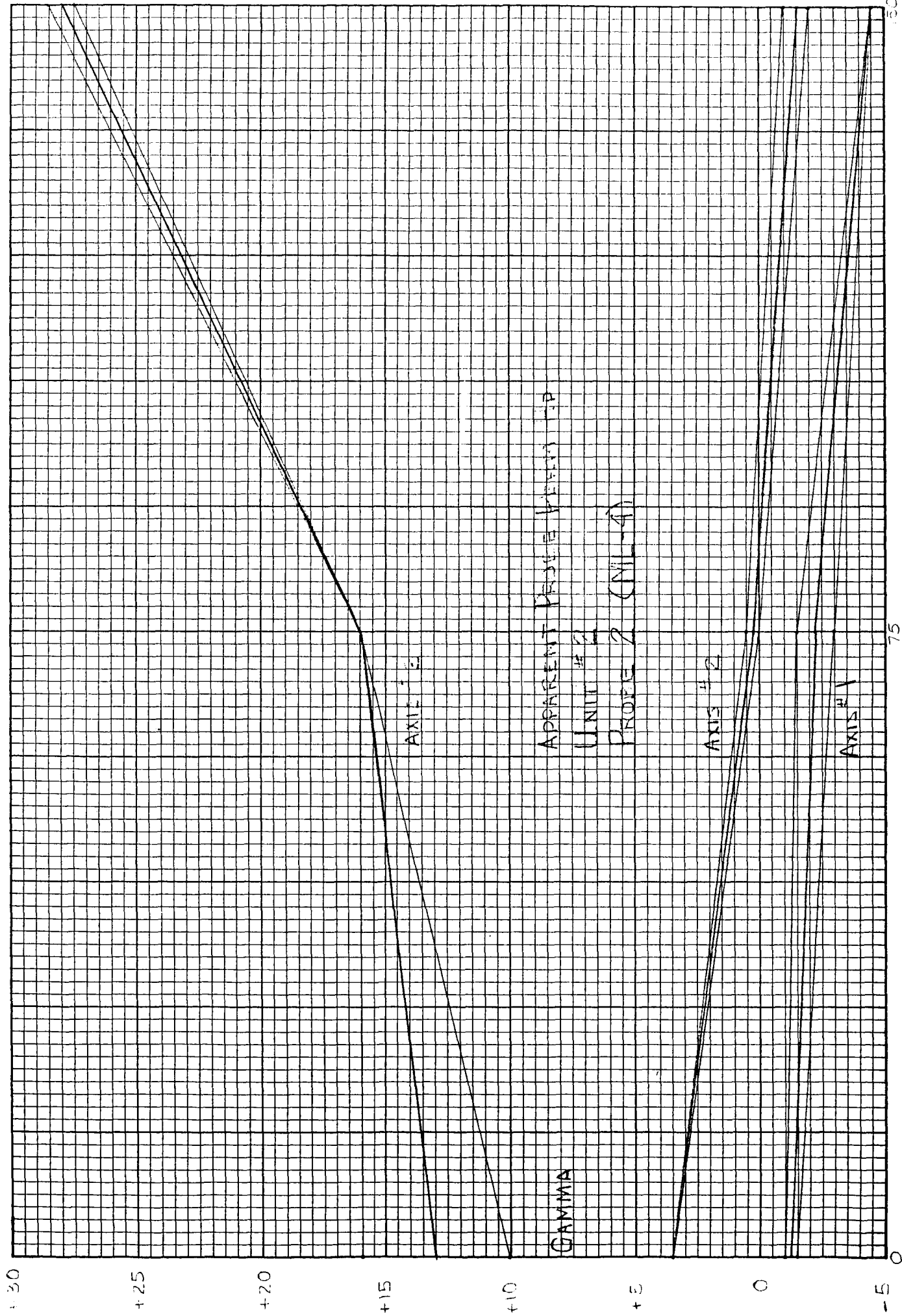


1-11-62





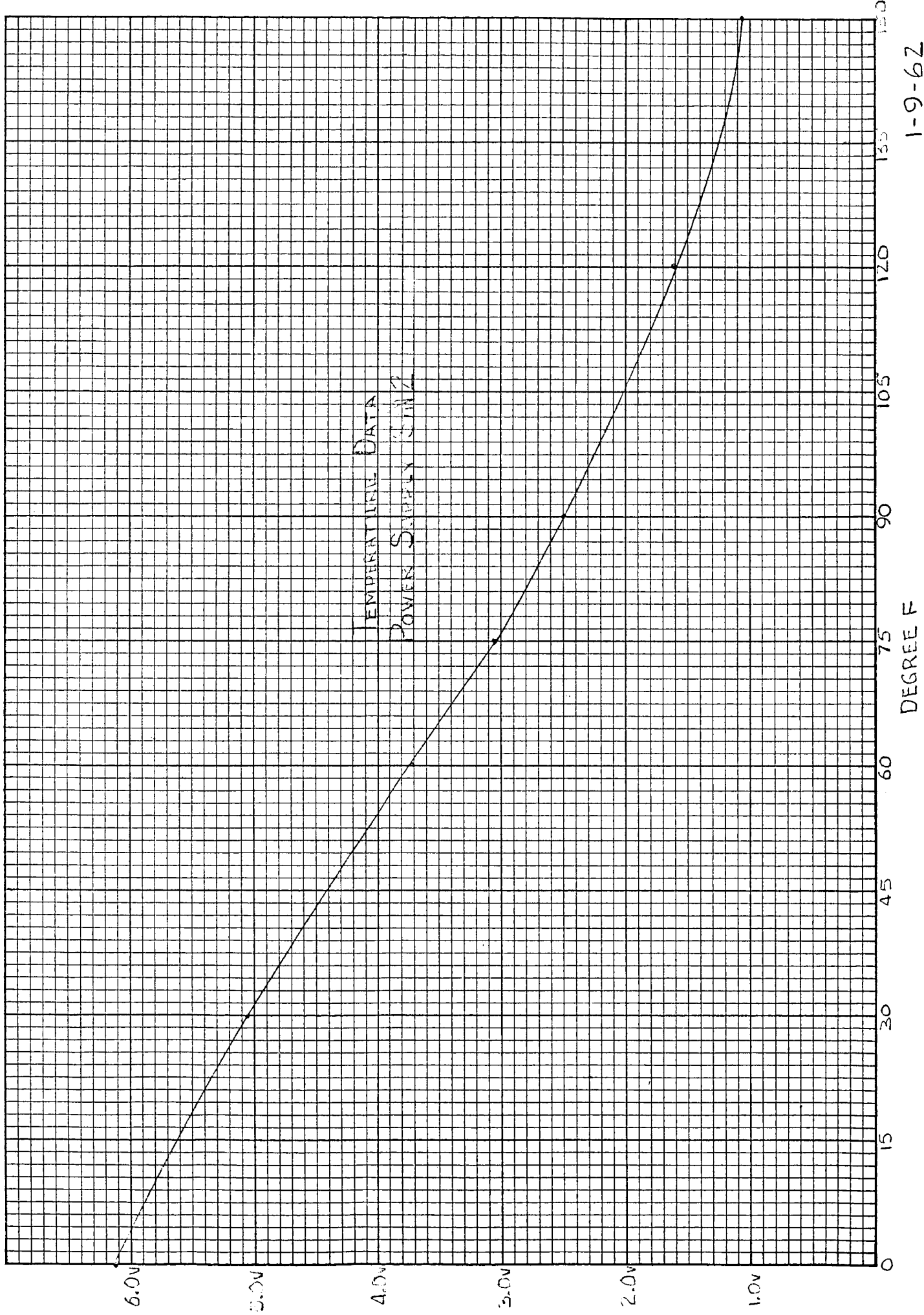




APPARENT RESISTANCE (P)
UNIT # 2
PROFE 2 (NL-4)

DEGREE F

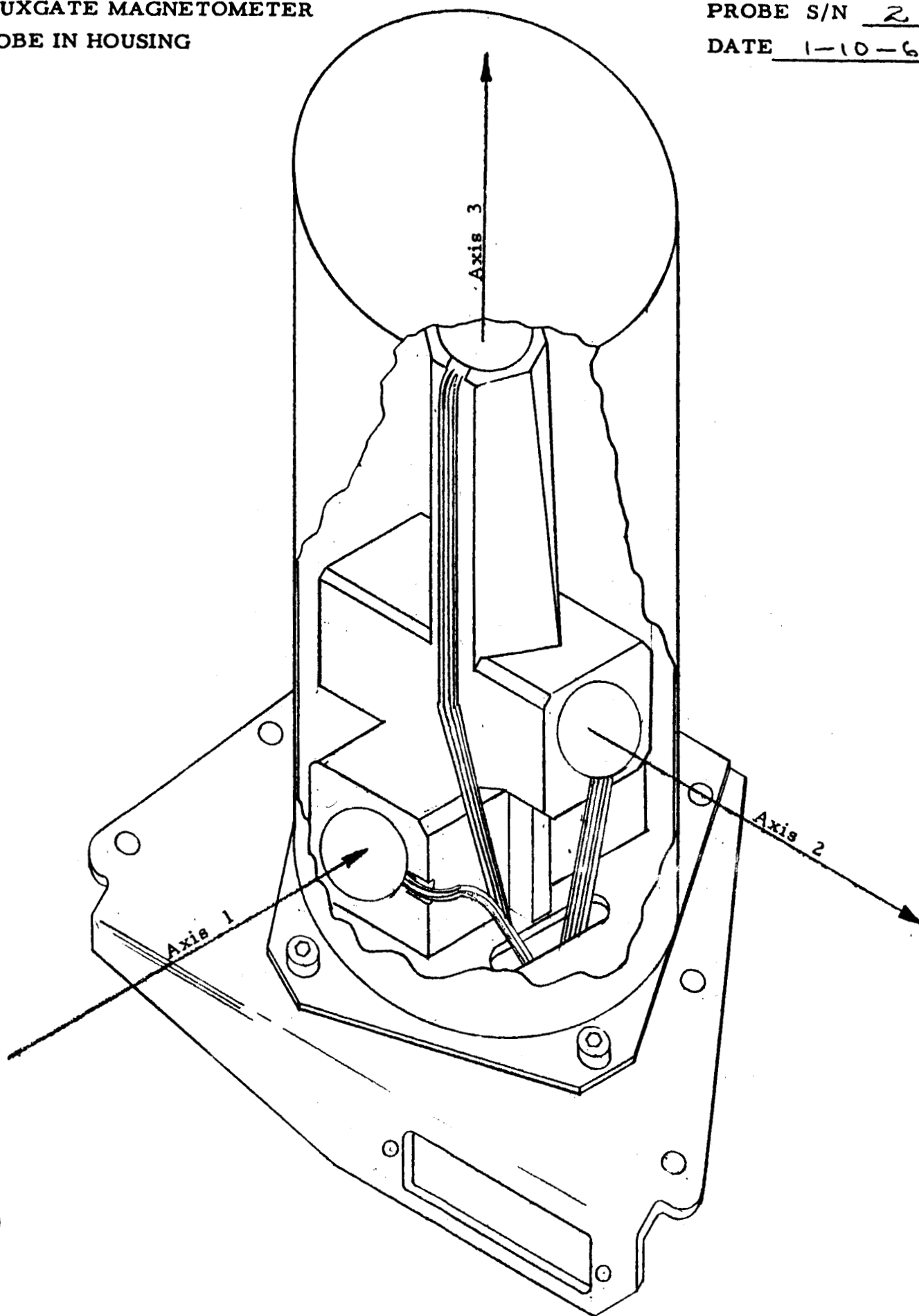
1-15-62



1-9-62

FLUXGATE MAGNETOMETER
PROBE IN HOUSING

PROBE S/N 2
DATE 1-10-62



Arrows indicate direction of magnetic force required to produce a positive output in the magnetometer, Mariner R, S/N 2.

MASTER DRAWING LIST

MARSHALL LABORATORIES

Triaxial Fluxgate Magnetometer

MODEL ML126-1

IDENTIFYING NAME

12-4-61

REVISION DATE

EFFECTIVITY

1 & UP

7 30 T 133HS

[illegible]

12-9-61 PREPARED BY Thompson

RELEASED

DEC 1 1961

MASTER DRAWING LIST

MARSHALL LABORATORIES

IDENTIFYING NAME Triaxial Fluxgate Magnetometer

IDENTIFYING NAME

ISSUE DATE 12-1-67

REVISION: DATE:

DATE _____

MODEL MTJ26-1

7 & 10

EFFECTIVITY

DATE _____

12-4-67

ISSUE DATE

[illegible]

Run 12-4-61

PREPARED BY:

Thompson

RELEASED

DEC 4 1961

MASTER DRAWING LIST

MARSHALL LABORATORIES

IDENTIFYING NAME Triaxial Fluxgate Magnetometer MODEL ML126-1

ISSUE DATE 12-4-61 REVISION DATE _____ EFFECTIVITY 1 & UP SHEET 3 OF 4

[illegible]

PREPARED BY Thompson

0.17-11-11

DEPT. OF JUSTICE

MASTER DRAWING LIST

DEC 4 1961

MARSHALL LABORATORIES

Triaxial Fluxgate Magnetometer

MODEL **ML126-1**

IDENTIFYING NAME

12-4-61

REVISION: DATE:

EFFECTIVITY

7 30 7 L33HS

LIST NO.	ASSEMBLY POSITION									DRAWING NUMBER	CHG. LIR.	DRAWING TITLE	NO. Shts.	Size
	1	2	3	4	5	6	7	8	9					
	X									50243-103		Circuit Board Assy. - Triaxial Fluxgate Mag.	1	J
			X							50242-101		Circuit Board	1	D
				X						50242-2		Board Assy.	1	D
					X					50242-1		Board Detail	1	D
REF						X				T50241		Circuit Master - Triaxial Fluxgate Mag.	2	J
							X			50242-3		Board Insulator	1	D
				X						SP30031-1		Transformer	1	D
				X						SP30001-4		Transformer	1	A
				X						SP30001-1		Transformer	1	A
				X						SP30001-3		Transformer	1	A
				X						SP30000-1		Inductor	1	A
				X						SP30002-3		Band Pass Filter	1	A
				X						F100-2		Bistable Multivibrator Module	1/2	C/A
				X						F603-2		Dual AC Emitter Follower Module	1/1	C/A
				X						F1000-2		Tuned Amp. Module	1/1	C/A
				X						F804-2		RC Amp Module	1/1	A/C
				X						F400-2		Trigger Module	1/1	A/C
				X						F502-3		Dual DC Inverter Module	1/1	A/C
				X						F400E-3		Fluxgate Special Module	1/1	A/C
				X						F900-2		RC Paraphase AMP. Module	1/1	A/C
				X						F1100-2		Push Pull Amp. Module	1/1	A/C
				X						F803-3		RC Amp. Module	1/1	A/C
				X						SP30061		Transistor	1	A

Run 12-4-61 PREPARED BY:

Thompson